http://pubsonline.informs.org/journal/ijoc/

INFORMS JOURNAL ON COMPUTING
Vol. 00, No. 0, Xxxxx 2018, pp. 1–22
ISSN 1091-9856 (print), ISSN 1526-5528 (online)

Exact Approaches for Network Design Problems with Relays

A1 Markus Leitner,[a] Ivana Ljubić,[b] Martin Riedler,[c] Mario Ruthmair[a]

[a] Department of Statistics and Operations Research, University of Vienna, 1010 Vienna, Austria; [b] ESSEC Business School of Paris, 95021 Cergy-Pontoise, France; [c] Institute of Logic and Computation, TU Wien, 1040 Vienna, Austria

Contact: markus.leitner@univie.ac.at, http://orcid.org/0000-0002-3313-9610 (ML); ljubic@essec.edu (IJ); riedler@ac.tuwien.ac.at (MartR); mario.ruthmair@univie.ac.at (MariR)

Received: January 5, 2016
Revised: September 20, 2017; February 27, 2018
Accepted: March 7, 2018
Published Online:

https://doi.org/10.1287/ijoc.2018.0820

Abstract. In this article we consider the network design problem with relays (NDPR), which gives answers to some important strategic design questions in telecommunication network design. Given a family of origin-destination pairs and a set of existing links these questions are as follows: (1) What are the optimal locations for signal regeneration devices (relays) and how many of them are needed? (2) Could the available infrastructure be enhanced by installing additional links in order to reduce the travel distance and therefore reduce the number of necessary relays?

In contrast to previous work on the NDPR, which mainly focused on heuristic approaches, we discuss exact methods based on different mixed-integer linear programming formulations for the problem. We develop branch-and-price and branch-price-and-cut algorithms that build upon models with an exponential number of variables (and constraints). In an extensive computational study, we analyze the performance of these approaches for instances that reflect different real-world settings. Finally, we also point out the relevance of the NDPR in the context of electric mobility.

History: Accepted by S. Raghavan, Area Editor for Network Optimization: Algorithms and Applications.

Funding: This work has been partly funded by the Vienna Science and Technology Fund (WWTF) through project ICT15-014. M. Leitner, I. Ljubić and M. Ruthmair are further supported by the Joint Programming Initiative Urban Europe and the Austrian Research Promotion Agency (FFG) [Grant 847350].

Keywords: A2 network design with relays • telecommunications • integer programming • branch and price

1. Introduction

A3 The network design problem with relays (NDPR) was introduced by Cabral et al. (2007) for modeling the design of telecommunication networks when the maximum distance a commodity (i.e., signal) can travel is bounded from above by some threshold and when distances exceeding this limit can be covered by locating special, commodity regenerating equipment (*relays*) at intermediate locations. Well-known applications in communication networks arise from signal deterioration and thus there is the need to regenerate them after some maximum distance by using rather expensive devices (e.g., repeaters); see, for example, Cabral et al. (2007). Without regeneration, the transmitted information might be falsified or the signal might be lost. As regeneration devices are usually expensive the goal is to use as few devices as possible (see Chen et al. 2010). As an alternative to placing relays the distance along certain connections may also be reduced by installing additional edges.

A4 **Problem Definition.** The network design problem with relays (NDPR) is defined on an undirected graph $G = (V, E, c, w, d)$ with relay costs $c\colon V \to \mathbb{N}_{>0}$, edge costs $w\colon E \to \mathbb{N}_{\geq 0}$, and edge lengths $d\colon E \to \mathbb{N}_{\geq 0}$. The edge set E is the disjoint union of the set of free (e.g., existing) edges $E^0 = \{e \mid w(e) = 0\}$ and the set of augmenting edges $E^* = \{e \mid w(e) > 0\}$. Furthermore, $\mathcal{K} \subseteq V \times V$ is the set of commodities. Parameter $d_{\max} \in \mathbb{N}_{>0}$ defines the maximum distance a commodity can traverse without regeneration.

The NDPR consists of selecting augmenting edges $\hat{E} \subseteq E^*$ to install and nodes $\hat{V} \subseteq V$ where relays are to be placed minimizing the resulting costs $\sum_{i \in \hat{V}} c_i + \sum_{e \in \hat{E}} w_e$. A solution is feasible iff all commodity pairs from $\mathcal{K}$ can communicate using the edges in $\hat{E} \cup E^0$ and relays at nodes $\hat{V}$. Thereby, two distinct nodes $s, t \in V$ can communicate if there exists a walk $W = (s = v_0, v_1, v_2, \ldots, v_k = t)$, $v_i \in V$, $0 \leq i \leq k$, that does not contain a subwalk $W' = (v_l, v_{l+1}, \ldots, v_{l+m})$, $0 \leq l \leq k-1$, $m \geq 0$, $l + m \leq k$, whose length $d(W') = \sum_{j=l}^{l+m-1} d_{j,j+1}$ is greater than $d_{\max}$ and that does not contain a relay at an intermediate node, that is, $v_j \notin \hat{V}$ for $l < j < l + m$. A walk satisfying these conditions is called a feasible walk and a feasible path is analogously defined.

An example of an NDPR instance together with an optimal solution is given in Figure 1.

Our Contribution and Structure of the Article. Available literature for the NDPR mainly deals with

Figure 1. An NDPR Instance and Its Optimal Solution for $d_{\max} = 4$ and $\mathcal{K} = \{(0,3),(0,4),(2,5),(3,4)\}$ in Which a Relay Is Installed at Node 1 and the Augmenting Edge $\{0,1\}$ Is Selected

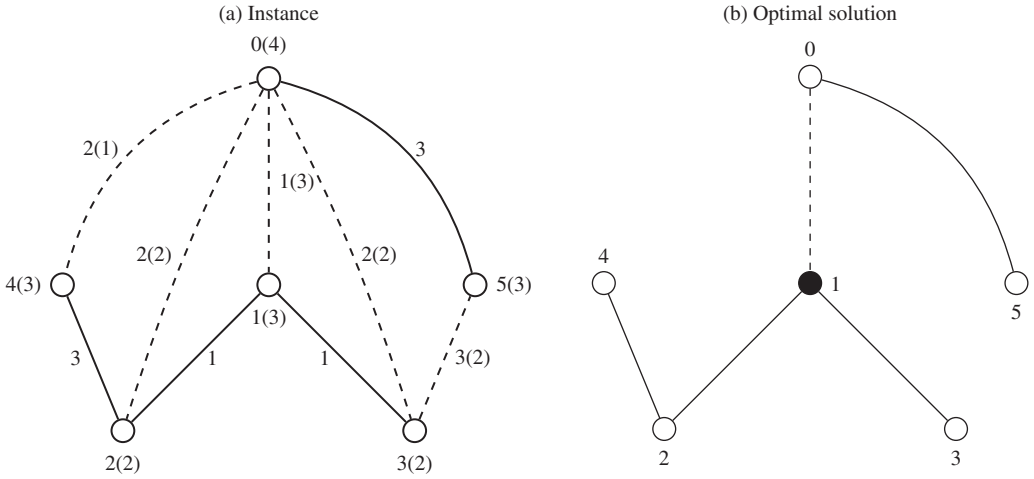

Notes. Nodes are labeled by node index and relay installation costs in parentheses. Edges are labeled by their lengths and installation costs in parentheses (for augmenting edges). Solid lines indicate free edges and dashed lines augmenting edges. Black nodes mark the selected relays in the solution.

heuristic approaches (see, e.g., Cabral et al. 2007, Kulturel-Konak and Konak 2008, Konak 2012). On the contrary, this article provides a comprehensive computational study of mixed-integer linear programming (MILP) models and underlying exact algorithms for the NDPR. A common characteristic of the presented MILP models is that they require an exponential number of variables representing paths in a so-called communication graph. The communication graph contains the same nodes as the original graph G and an edge between every two nodes that can be connected via a feasible path without installing relays.

For deriving computationally viable optimization tools for the proposed MILP models, we implemented two branch-price-and-cut algorithms. Their performance is assessed on a large set of benchmark instances—some of them taken from the available literature, and some newly generated ones.

The article is organized as follows. In the remainder of this section we summarize our notation and provide an overview of the related literature. In Section 2 we prove some structural properties of feasible/optimal solutions that will help us to create tighter formulations. In Section 3 we discuss transformations of the input graph and associated MILP formulations. Section 4 provides the details of our algorithmic framework followed by the presentation of our computational results on a diverse family of benchmark instances in Section 5. Finally, we discuss challenges and open questions for further research in Section 6 where we also summarize our main conclusions.

1.1. Notation and Assumptions

To ease notation in many of the results and formulations introduced in the following, we will consider the node pairs (i.e., commodities) to be directed pairs $(u,v) \in \mathcal{K}$. This assumption is without loss of generality, since there are no costs or capacities associated with the routing decisions in the NDPR. Furthermore, we define the set of *sources* $\mathcal{K}^{\mathrm{S}} = \{u \mid \exists\, v \in V \text{ such that } (u,v) \in \mathcal{K}\}$ and the set of targets $\mathcal{K}^{\mathrm{T}}_u = \{v \mid (u,v) \in \mathcal{K}\}$ that have to be reached by source $u \in \mathcal{K}^{\mathrm{S}}$. Similarly, the set of all *targets* is defined as $\mathcal{K}^{\mathrm{T}} = \{v \mid \exists\, u \in V \text{ such that } (u,v) \in \mathcal{K}\} = \bigcup_{u \in \mathcal{K}^{\mathrm{S}}} \mathcal{K}^{\mathrm{T}}_u$.

Let $\delta(S) = \{\{i,j\} \in E \mid i \in S, j \in V \setminus S\}$ denote the set of edges incident to $S \subseteq V$ in the undirected graph $G = (V,E)$. For a directed graph $G' = (V',A')$ and node subset $S \subseteq V'$, we define $\delta^+(S) = \{(i,j) \in A' \mid i \in S, j \in V \setminus S\}$ and $\delta^-(S) = \{(i,j) \in A' \mid i \in V \setminus S, j \in S\}$ as the set of outgoing and incoming arcs, respectively.

Finally, observe that edges $e \in E$ such that $d_e > d_{\max}$ as well as commodities $(u,v) \in \mathcal{K}$ for which G contains a feasible path between the endpoints, using free edges from E^0 only and no relays, can be removed in a preprocessing step. Thus, we assume without loss of generality that neither of them exists in the given input.

1.2. Related Work and Applications in Transportation

The NDPR was introduced by Cabral et al. (2007) who showed that the problem is NP-hard and described heuristic approaches intended to solve large instances. Furthermore, an MILP formulation of the problem based on an exponential number of variables is described. Contrary to our path variables derived in the communication graph (cf. Section 3.1), Cabral et al. (2007) use variables representing entire walks between the commodities in the original graph (including the placement of relays). Their formulation is used to derive lower bounds by means of column generation.

At the same time, the subset of generated columns is used to compute heuristic solutions in a subsequent branch-and-bound phase. Computational results are discussed for instances with up to 62 nodes, 103 edges, and 10 commodities.

A hybrid metaheuristic combining a genetic algorithm with local search has been proposed by Kulturel-Konak and Konak (2008) whereas an improved genetic algorithm is given in Konak (2012). In the latter article, Konak also introduces a variant of the MILP formulation by Cabral et al. (2007) by using separate variables to represent walks and relay placements. However, no computational studies concerning this model were conducted. Instead, some observations regarding the set covering constraints introduced in this formulation are used in the design of the proposed genetic algorithm. Computational results are given on instances with up to 160 nodes and 3,624 edges and 10 commodities. Lin et al. (2014) proposed a tabu search approach for the NDPR. Their solution method computes solutions of almost as good quality as the genetic algorithm from Konak (2012) but requires less computing time. Very recently, Xiao and Konak (2017) presented a variable neighborhood search for the NDPR that is combined with an exact algorithm for the relay placement. Independently from our work an alternative branch-and-price approach was developed in Yıldız et al. (2018). The authors propose MILP formulations on a so-called virtual network with an exponential number of edges. Their computational study mainly focuses on a tree formulation specifically designed for the single source case, that is, $|\mathcal{K}^S| = 1$.

A related version of the NDPR, defined on a directed graph and called the directed network design problem with relays (DNDPR), has been introduced in Li et al. (2012) where a compact MILP model and a branch-and-price algorithm have been proposed. The problem definition is however slightly different from the NDPR: in the DNDPR only simple paths are allowed for connecting commodity pairs, whereas the NDPR also allows using walks. In fact, allowing multiple node visits in general makes NDPR solutions significantly less expensive than DNDPR solutions; see Section 2 for further details. The compact formulation given in Li et al. (2012) exploits the fact that, along a path connecting a commodity pair, each node can be visited at most once. More precisely, it uses a single variable per node to record the distance from the source at which it is reached. Consequently, this formulation cannot be used for solving the NDPR. Their branch-and-price algorithm, which is very similar to the one considered by Cabral et al. (2007), is in general capable of allowing cycles but in the computational experiments the authors only consider the acyclic case. Finally, Kabadurmus and Smith (2015) study an extension of the NDPR that considers survivability, edge capacities, and allows for k-splitting of the routes of a commodity.

Application in Transportation. Yıldız and Karaşan (2015) provide a detailed survey on applications of relay placement problems in transportation. In some of these applications dealing with hub location issues, hubs are interpreted as relays, that is, the location of hubs naturally corresponds to the placement of relays. The underlying problems are concerned with identifying physical locations of hubs that may serve as places for the exchange of drivers, trucks, and trailers, or as stations where drivers can rest (cf. Üster and Kewcharoenwong 2011, Campbell and O'Kelly 2012). Moreover, hubs can be used for switching transportation means or simply for storing the consignment to be picked up by other drivers (see Üster and Maheshwari 2007). Since certain road sections might be more costly to use (e.g., if additional tolls need to be paid) or certain possibilities to extend the road network might exist, the consideration of edge selection is relevant as well. The placement of refueling stations for alternative-fuel vehicles is another important area where the NDPR arises as a subproblem. The distance constraints considered in the NDPR are well motivated by the typical range restrictions of such vehicles; see, for example, Schneider et al. (2014) and the survey by Pelletier et al. (2016).

Additionally, we want to point out the relation to the so-called minimum cost path problem for plug-in hybrid electric vehicles (PHEV) considered by Arslan et al. (2015). In this problem a PHEV needs to travel from an origin to a destination node using gasoline refueling and electric charging stations while minimizing refueling, charging, and traveling costs. The authors solve the problem with a mixed-integer quadratically constrained formulation. The considered problem is very similar to the NDPR. The charging stations can be viewed as some kind of relays and the vehicle corresponds to a single commodity. The primary difference lies in the fact that refueling and charging stations need to be modeled as two different types of relays that introduce additional complexity. Nevertheless, solution techniques introduced in this paper for the NDPR (in particular, the modeling of path segments between two consecutive charging stations and the generation of the communication graph) might also be relevant for solving the PHEV problem. The placement of refueling stations has also been considered in Capar et al. (2013) and Yıldız et al. (2016) where the goal is to select locations for the refueling stations such that the total volume of the refueled demand is maximized for a given set of origin-destination pairs. Yıldız et al. (2016) solve the problem with a branch-and-price approach that uses an exponential number of path variables to model route feasibility.

Relation to Regenerator Location/Placement Problems. The regenerator location problem (RLP) introduced by Chen et al. (2010) is closely related to the NDPR but focuses on the placement of regenerators (relays) and no additional edges can be purchased/installed in the network. More precisely, the RLP is a special case of the NDPR for $E^* = \emptyset$ and $\mathcal{K} = \{(u,v) \mid u,v \in V\, u < v\}$, that is, it is assumed that all edges have zero costs and all node pairs need to communicate. As the RLP is equivalent to the maximum leaf spanning tree problem (MLSTP) and the minimum connected dominating set problem (MCDSP) (see, e.g., Lucena et al. 2010, Gendron et al. 2014) the NDPR generalizes these problems as well. Chen et al. (2010) provide several MILP formulations for the RLP, which unfortunately cannot be directly used to solve the NDPR since they are not capable of selecting augmenting edges. We will, however, use the concept of a communication graph provided in Chen et al. (2010) for solving the NDPR; cf. Section 3.1 for a detailed description. Further exact approaches for the RLP have been developed by Rahman et al. (2015), who propose compact formulations and branch-and-cut algorithms. In a recent contribution by Yıldız and Karaşan (2015), survivability requirements are added to the RLP.

Chen et al. (2015) introduced the so-called generalized regenerator location problem (GRLP), which extends the RLP by considering node sets $S \subseteq V$ of potential relay locations and $T \subseteq V$ of terminal nodes that need to be able to communicate with each other, that is, $\mathcal{K} = \{(i,j) \mid i,j \in T, i < j\}$. Again, the proposed models for the GRLP cannot be applied to the NDPR. On the other hand, the NDPR is able to model the GRLP by assigning infinite costs to the nodes in $V \setminus S$ or by adding constraints that prohibit that the nodes in $V \setminus S$ are chosen as relays. The latter can be easily done in all formulations that will be introduced in the following.

Another recent contribution by Yıldız and Karaşan (2017) considers several practical extensions like routing, bandwidth allocation, and modulation selection. The proposed flow model uses an exponential number of variables and is solved by a branch-and-price approach. Finally, in a broader sense, the NDPR is also related to optimization problems dealing with wavelength division multiplexing, but, in contrast to the NDPR, the routing of an optical signal has to be optimized at two layers, the logical and the physical one (see, e.g., Raghavan and Stanojević 2011, Sung and Song 2003, for further details).

2. Solution Properties

In this section we introduce and prove certain structural properties of optimal NDPR solutions that will be used to derive MILP formulations in the next section. Recall that a solution consists of a subset $\hat{E} \subseteq E^*$ of augmenting edges (together with the free edges E^0), and a subset $\hat{V} \subseteq V$ of nodes where relays have to be installed.

As previously mentioned, commodity pairs $(u,v) \in \mathcal{K}$ are assumed to be ordered, so that routing a signal from u to v is determined by a feasible (directed) u,v-walk embedded in the subgraph induced by $\hat{E} \cup E^0$, and using a subset of relays from the set $\hat{V}$. Hence, even though the solution corresponds to an undirected graph (along with the placement of relays), routing decisions are given by directed walks that are incorporated in the solution graph. In our terminology, a feasible walk corresponds to a directed subgraph embedded in the undirected solution graph, so that each edge can be traversed in both directions. The number of visits of a node in a feasible walk is equal to the in-degree of this node in the associated directed graph.

To better illustrate this interplay between the undirected solution graph and the directed subgraph associated with the routing decisions, let us consider the instance given in Figure 2(a) and assume $d_{\max} = 4$ and $\mathcal{K} = \{(0,3)\}$. The unique optimal solution, which is visualized in Figure 2(b), selects all edges and places a relay at node 2. The routing of a signal from node 0 to node 3 is given by a directed walk $(0,1,2,1,3)$ embedded in this solution. This walk traverses the edge $\{1,2\}$ twice and visits node 1 twice forming a cycle; cf. Figure 2(c). Notice that the definition of the NDPR does not forbid such cycles. As a matter of fact,

Figure 2. Example Instance with a Cyclic Solution for $d_{\max} = 4$ and $\mathcal{K} = \{(0,3)\}$

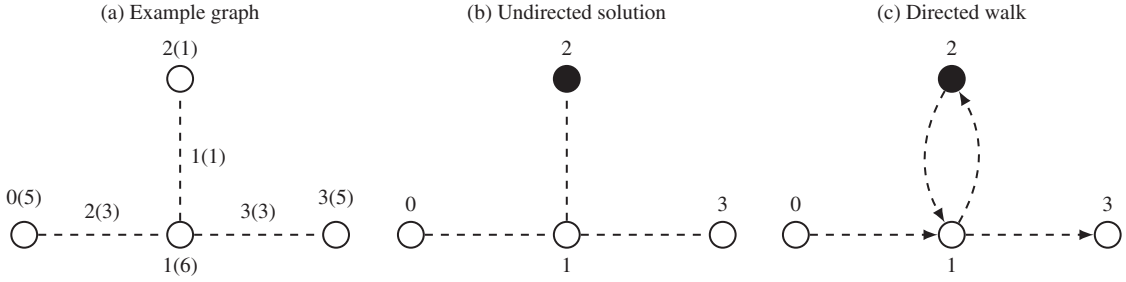

Notes. Nodes are labeled by node index and relay installation costs in parentheses. Augmenting edges are labeled by their lengths and installations costs in parentheses. Dashed lines indicate augmenting edges. Black nodes mark the selected relays in the solution.

enforcing that each commodity is connected by a (simple) path might significantly increase the cost of a solution. In the considered example a relay would need to be placed at node 1 instead of at 2 and edge $\{1,2\}$ would not be traversed. Consequently, the solution cost would increase from 8 to 12.

In the following, we focus on structural properties dealing with routing decisions in an optimal NDPR solution. We first prove two properties that are concerned with the maximum number of node visits for connecting a single commodity before we show that analogous results also hold when simultaneously considering all commodities with a common source.

Property 1. *In every optimal solution there exists for every pair $(u,v) \in \mathcal{K}$ a feasible walk from u to v visiting each relay at most once.*

Proof. Let $W = (u, w_0, i, w_1, i, \dots, w_{n-1}, i, w_n, v)$ be a feasible u,v-walk in an optimal solution that consists of subwalks $\{w_0, w_1, \dots, w_n\}$ with $i \in V$, $i \neq u, v$; cf. Figure 3. If i is a relay node, then walk $W' = (u, w_0, i, w_n, v)$ visiting node i only once clearly is a feasible u,v-walk as well. By repeating this argument, we will end up with a feasible u,v-walk in which each relay node appears at most once. □

Property 2. *In every optimal solution there exists for every pair $(u,v) \in \mathcal{K}$ a feasible walk from u to v visiting each nonrelay node at most twice.*

Proof. Let $i \in V$ be the nonrelay node closest to u, which is visited $n > 2$ times in a feasible u,v-walk. Let the feasible u,v-walk be represented as $W = (u, w_0, i, w_1, i, \dots, w_{n-1}, i, w_n, v)$ with subwalks $\{w_0, w_1, \dots, w_n\}$ that do not visit i; cf. Figure 3. Clearly, each subwalk w_ℓ $(1 \le \ell \le n-1)$ that contains no relays, can be deleted from W without violating feasibility. Hence, let us assume that at least one relay is traversed in w_ℓ, for all $1 \le \ell < n$, and let $r \in V$ be the relay node with minimum distance from/to i in any of the subwalks $w_1, \dots w_n$ (considered undirected). Let $(i, v_0, v_1, \dots, v_l = r)$, $v_k \neq i$, $0 \le k \le l$, be the corresponding path from i to r with minimum length. Then, $W' = (u, w_0, i, v_0, v_1, \dots, v_l = r, v_{l-1}, \dots, v_0, i, w_n, v)$ is a feasible u,v-walk visiting i exactly two times. By repeating this procedure for each nonrelay node that is visited more than twice, we can construct a feasible walk with the desired property. □

Figure 3. Path from u to v Visiting Node i n Times

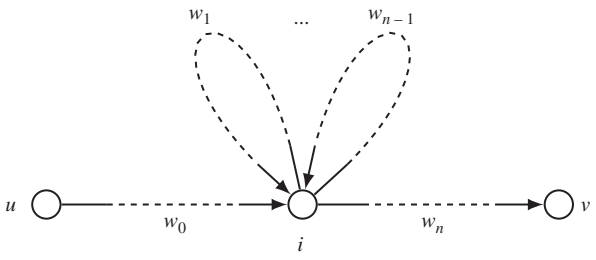

Definition 1. A feasible walk w connecting a commodity pair $(u,v) \in \mathcal{K}$ is called *nonredundant* if it does not contain a feasible u,v-subwalk w', $w' \neq w$.

Remark 1. Every nonredundant walk satisfies Properties 1 and 2. If a nonrelay node is visited twice in a nonredundant walk, then the second visit occurs in terms of a cycle that visits a relay. Each feasible walk can be converted into a nonredundant one using the reduction techniques from the proofs of Properties 1 and 2.

Theorem 1. *Given a source $u \in \mathcal{K}^S$, in every optimal solution one can embed a digraph rooted at u containing a feasible walk from u to every target $v \in \mathcal{K}_u^T$. In this digraph, each relay has in-degree at most one and each nonrelay node has in-degree at most two.*

Proof. We show the existence of such a digraph $\tilde{G}$ by construction. According to Properties 1 and 2, for each target $v \in \mathcal{K}_u^T$ there exists a feasible walk from u to v with the desired properties. We choose one of the targets $v \in \mathcal{K}_u^T$ and initialize the graph $\tilde{G}$ with arcs determining its feasible walk (satisfying Properties 1 and 2). We then continue to iteratively insert nonredundant walks for the remaining targets. Whenever a new walk (associated with a new target) is considered, there are three possibilities: (a) the graph already contains the walk's target, (b) the graph and the walk are node-disjoint (except for the source u), or (c) the graph and the walk share more than one node.

If (a) occurs, we do not modify $\tilde{G}$ and continue with the next target node. Case (b) allows to add the walk to $\tilde{G}$ without violating the desired properties since the in-degrees of nodes already existing in $\tilde{G}$ do not change. The third case (c) is more difficult to handle since simply adding the walk might increase the in-degree for some nodes and thus can destroy the properties we need.

Initially we add the walk to $\tilde{G}$. Let $Z = \{z_1, \dots, z_n\}$ be the set of nodes on this walk with in-degree greater than one. Each of these nodes might be in conflict with the required properties. To resolve this issue we apply a pruning procedure to each node $z \in Z$.

First, we identify a nonredundant walk in $\tilde{G}$ that reaches z at minimum distance (using as few edges as possible) from the preceding relay or node u. This walk might visit z at most twice using a cycle to a relay to reduce the distance. Then, we delete all incoming arcs of z not contained in this walk. Moreover, we iteratively remove preceding arcs of the already removed ones (not contained in the walk) until we arrive at source node u, a node that is a target, or a node that has an outgoing walk to a target. For an example see Figure 4.

After processing all u,v-walks in this way we can reach all targets of u in $\tilde{G}$. Moreover, walks are added such that all nodes in $\tilde{G}$ are guaranteed to meet the required degree restrictions. □

Figure 4. (Color online) A Directed Graph Rooted at u That Needs to Reach Targets $\mathcal{K}_u^{\mathrm{T}} = \{v, v', v''\}$

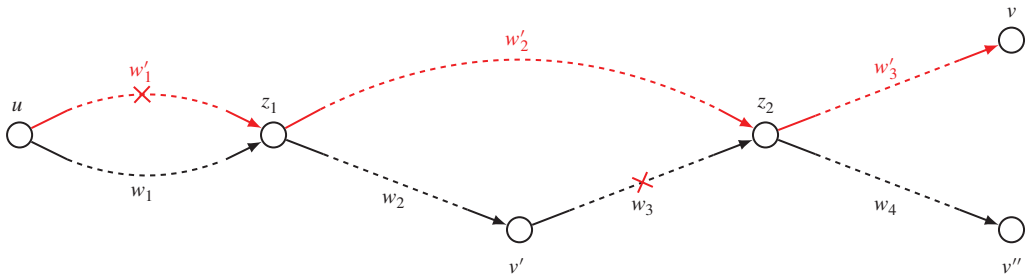

Notes. We illustrate the pruning procedure after adding the red walk to the current digraph $\tilde{G}$ shown in black. The pruning procedure applied to nodes z_2 and z_1 removes subwalks w_3 and w'_1, respectively.

3. Mixed-Integer Linear Programming Formulations

The MILP formulations that will be introduced in the following are based on a *communication graph* whose construction from the original graph will be explained next. Afterward, we will provide two MILP formulations and discuss their properties.

3.1. Communication Graph

Communication graph $G_C = (V, C)$ is defined on the original node set V and its edge set C consists of all node pairs $\{i, j\} \subseteq V$, $i \neq j$, for which at least one path P with length $d(P) \leq d_{\max}$ exists in G, that is, i and j can communicate using edges from E^* or E^0 without installing relays. Recall that (after preprocessing) every feasible path without relays connecting commodity $(u, v) \in \mathcal{K}$ in G contains at least one edge $e \in E^*$ with positive costs. Since multiple paths can be used for connecting a node pair, it is not clear which one of the potentially exponentially many paths will be used in an optimal solution and thus all of them need to be considered. Our definition of the communication graph extends the one introduced in Chen et al. (2010 and 2015) for solving the (G)RLP. In contrast to their definition, our communication graph considers all edges $e \in E$ and not only those with zero costs.

Figure 5 demonstrates how the existence of common subpaths for several commodities produces a better solution than the one obtained by combining cheapest subpaths of the individual commodities. Assume $\mathcal{K} = \{(0,2),(0,3)\}$ and observe that the cheapest $0,2$-path is the edge $\{0,2\}$ and the cheapest $0,3$-path is edge $\{0,3\}$, both with a cost of 2 yielding a solution with total cost 4. The union of paths $(0,1,2)$ and $(0,1,3)$ results, however, in a cheaper solution with total cost 3.

In the following, for each pair of distinct nodes $b = \{i, j\}$, let $P_b = \{p \mid p \text{ is an } i,j-\text{path in } G, \text{ such that } d(p) \leq d_{\max}\}$ be the set of all feasible i,j-paths in G. Furthermore, let $P_b^0 = \{p \mid p \text{ is an } i,j-\text{path in } G^0, \text{ such that } d(p) \leq d_{\max}\}$ be the set of all such paths in $G^0 = (V, E^0)$, that is, using only free edges. Then, sets $C^0 = \{b = \{i, j\} \mid P_b^0 \neq \varnothing\}$ and $C^* = \{b = \{i, j\} \mid P_b^0 = \varnothing \text{ and } P_b \neq \varnothing\}$ define the node pairs that can be connected using only free edges and using at least one augmenting edge, respectively. Thus, the edge set C of communication graph $G_C = (V, C)$ corresponding to $G = (V, E)$ is defined as $C = C^* \cup C^0$, that is, the set of node pairs that can be connected using edges in $E^* \cup E^0$.

Figure 6 illustrates the stepwise generation of a communication graph for the input graph provided in Figure 6(a), $d_{\max} = 4$. After initializing C with the set of free edges E^0, all remaining edges $C^0 \backslash E^0$ corresponding to connections that can be established by using only free edges and no relays are added; cf. the edges $\{1,4\}$ and $\{2,3\}$ corresponding to paths $(1,2,4)$ and $(2,1,3)$, respectively, in Figure 6(b). Next, all connections possible through the use of augmenting edges (i.e., either augmenting edges or paths containing at least one augmenting edge) are considered; see the dashed edges in Figure 6(c). The corresponding node pairs are connected by dotted lines in Figure 6(c). Communication graph G_C is finally obtained by removing potentially existing multiedges; cf. Figure 6(d) where connections

Figure 5. Shortest Path Connections May Be Suboptimal Because of Edge Reuse

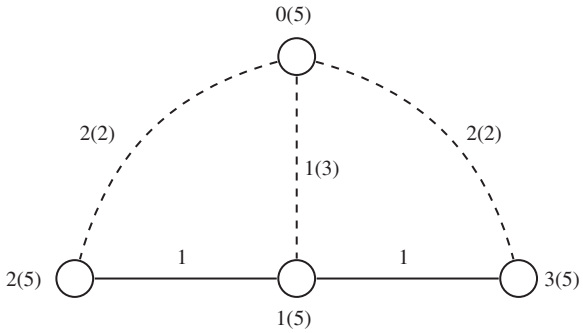

Notes. Paths $(0,1,2)$ and $(0,1,3)$ are dominated by $(0,2)$ and $(0,3)$, respectively. Nevertheless, the optimal solution is $\{\{0,1\},\{1,2\},\{1,3\}\}$ ($\mathcal{K} = \{(0,2),(0,3)\}$ and $d_{\max} = 3$). Nodes are labeled by node index and relay installation costs in parentheses. Edges are labeled by their lengths and installation costs in parentheses (for augmenting edges). Solid lines indicate free edges and dashed lines augmenting edges.

Figure 6. Generation of the Communication Graph for $d_{\max} = 4$

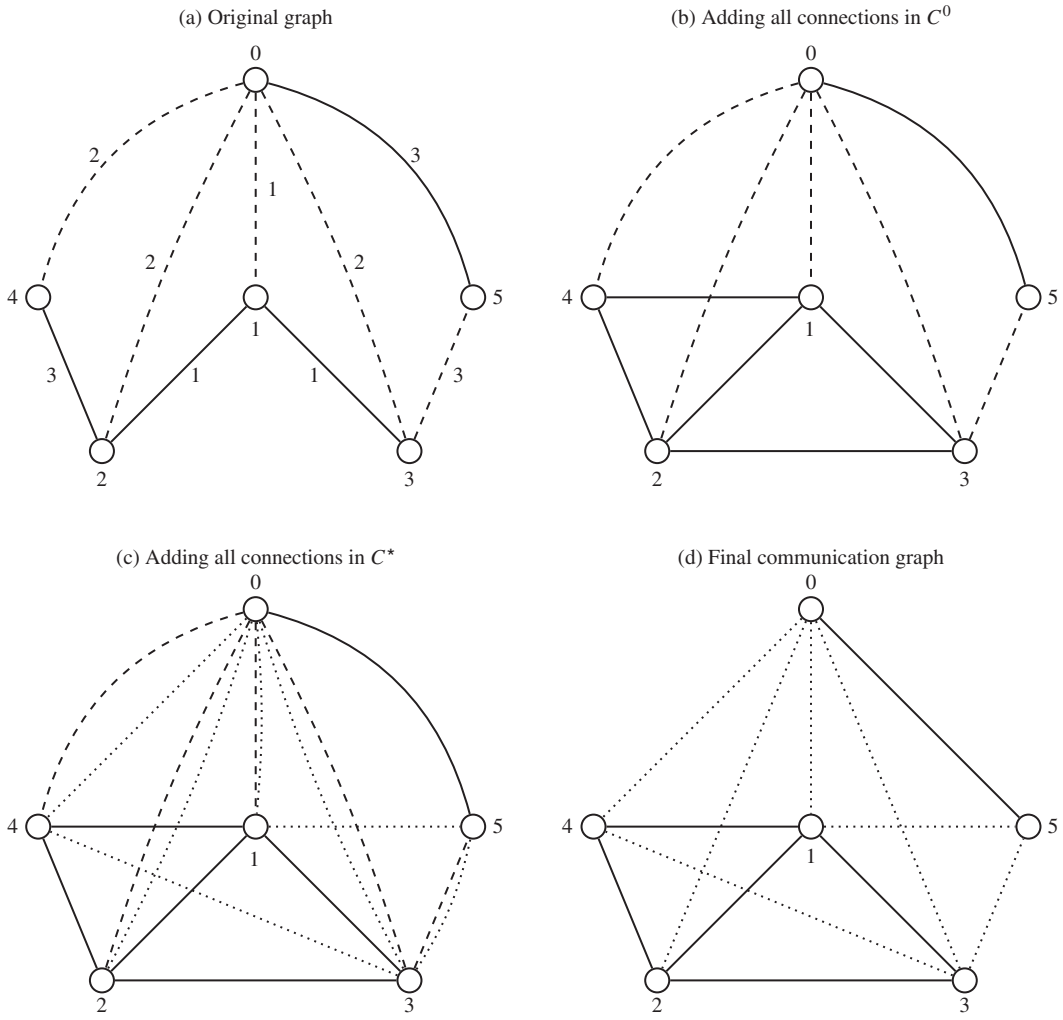

Notes. Nodes are labeled by node index. Edges are labeled by their lengths. Solid lines indicate free edges, dashed lines augmenting edges, and dotted lines indicate connections from C^*.

in C^0 and C^* are displayed by solid and dotted lines, respectively.

The following property of the communication graphs is crucial for developing the MILP models shown later.

Property 3. *For every commodity pair $(u, v) \in \mathcal{K}$, a nonredundant u, v-walk in the original graph can be mapped to a simple path in the communication graph with relays placed at all intermediate nodes (if any).*

Proof. According to Remark 1 there exists a nonredundant (feasible) walk in the original graph visiting every relay at most once. Observe that we can partition the walk in the original graph into maximal feasible subwalks such that none of their intermediate nodes are relays. Communication graph G_C contains an edge for every feasible path that is not required to visit any relays. Therefore, the mentioned subwalks can be translated to edges of the communication graph leading to the desired simple path. Conversely, each simple path in the communication graph can be translated to a nonredundant path in the original graph. □

Corollary 1. *For a feasible solution, we can identify for each source $u \in \mathcal{K}^S$ and all its targets a tree in the communication graph with relays placed at all intermediate nodes where each leaf is a target of u such that each (unique) path to a target corresponds to a feasible walk in the original graph.*

Proof. We use the graph obtained according to the proof of Theorem 1. Then, we partition and translate it in the same way as in the proof of Property 3. □

The MILP formulations introduced in the following sections make use of flows or cut sets to model feasible paths in the communication graph. In addition, the relation between edges in G_C and (an exponential number of) paths in G is established.

3.2. Multicommodity Flow Formulation

We first present a multicommodity flow formulation on the communication graph (MCF), which uses one

set of flow variables for each commodity in $\mathcal{K}$. It utilizes the following design variables defined on G:

$$x_e = \begin{cases} 1, & \text{if } e \text{ is installed in the network} \\ 0, & \text{otherwise} \end{cases} \quad \forall e \in E^*$$

$$y_i = \begin{cases} 1, & \text{if a relay is installed at } i \\ 0, & \text{otherwise} \end{cases} \quad \forall i \in V.$$

Using $A(C) = \{(i,j) \mid \{i,j\} \in C\}$ we define flow variables f_{ij}^{uv} for all commodity pairs $(u,v) \in \mathcal{K}$ and each direction of edge $\{i,j\} \in C$, that is,

$$f_{ij}^{uv} = \begin{cases} 1, & \text{if the } u,v\text{-path in } G_C \\ & \quad \text{traverses edge } \{i,j\} \\ & \quad \text{in direction from } i \text{ to } j \\ 0, & \text{otherwise} \end{cases} \quad \forall (i,j) \in A(C).$$

Finally, we use variables λ_b^p that correspond to the paths $p \in P_b$ that have been identified as possible realizations for the connections $b \in C^*$. More precisely,

$$\lambda_b^p = \begin{cases} 1, & \text{if connection } b \text{ is realized} \\ & \quad \text{by path } p \in P_b \\ 0, & \text{otherwise} \end{cases} \quad \forall b \in C^*.$$

Since no augmenting edges need to be purchased when sending flow through edges from C^0, we do not need to consider path variables for $b \in C^0$. The MILP formulation reads as follows:

$$\text{(MCF)} \quad \text{minimize} \sum_{i \in V} c_i y_i + \sum_{e \in E^*} w_e x_e \tag{1}$$

$$\sum_{(i,j) \in A(C)} f_{ij}^{uv} - \sum_{(j,i) \in A(C)} f_{ji}^{uv} = \begin{cases} 1 & i = u \\ -1 & i = v \\ 0 & i \neq u,\ i \neq v \end{cases} \quad \forall (u,v) \in \mathcal{K},\ \forall i \in V \tag{2}$$

$$-y_i + \sum_{(i,j) \in A(C)} f_{ij}^{uv} \leq 0 \quad \forall (u,v) \in \mathcal{K},\ \forall i \in V \setminus \{u,v\} \tag{3}$$

$$-(f_{ij}^{uv} + f_{ji}^{uv}) + \sum_{p \in P_b} \lambda_b^p \geq 0 \quad \forall (u,v) \in \mathcal{K},\ \forall b = \{i,j\} \in C^* \quad (\mu_b^{uv}) \tag{4}$$

$$x_e - \sum_{p \in P_b : e \in p} \lambda_b^p \geq 0 \quad \forall e \in E^*,\ \forall b \in C^* \quad (\alpha_b^e) \tag{5}$$

$$\lambda_b^p \geq 0 \quad \forall b \in C^*,\ p \in P_b \tag{6}$$

$$0 \leq f_{ij}^{uv} \leq 1 \quad \forall (u,v) \in \mathcal{K},\ \forall (i,j) \in A_C \tag{7}$$

$$\mathbf{y} \in \{0,1\}^{|V|},\ \mathbf{x} \in \{0,1\}^{|E^*|}. \tag{8}$$

Constraints (2) ensure that for each commodity $(u,v) \in \mathcal{K}$ one unit of flow is sent from u to v. Every node with outgoing flow that is not the source of the corresponding flow must be a relay node; cf. Property 3. This relation is enforced by inequalities (3). Constraints (4) ensure that flow along a connection $b \in C^*$ is only permitted if at least one of the available path realizations has been selected. Due to Property 3, the solution for each commodity pair $(u,v) \in \mathcal{K}$ will be a path in G_C. Hence, only one arc (i,j) or (j,i) per edge $b = \{i,j\}$ will be selected in each variable set. The last set of inequalities guarantees that for all selected path realizations, the corresponding augmenting edges will be part of the solution. Note that each variable set only considers a single pair $(u,v) \in \mathcal{K}$. Arcs targeting u or leaving v are irrelevant with respect to the flow variables, hence the respective flow variables can be omitted from the formulation.

Pricing Subproblem. Since the number of path variables in formulation (MCF) may be exponentially large we will use column generation for solving its linear programming (LP) relaxation. To formulate the pricing subproblem, let $\mu_b^{uv} \geq 0$ and $\alpha_b^e \geq 0$ be the dual variables associated to constraints (4) and (5), respectively. Then, for each $b \in C^*$, the pricing subproblem (i.e., find a path $p \in P_b$ with negative reduced costs) is defined as

$$\arg\min_{p \in P_b} \left(\sum_{e \in E^* \cap p} \alpha_b^e - \sum_{(u,v) \in \mathcal{K}} \mu_b^{uv} \right).$$

Since the second summation is a constant for a fixed $b \in C^*$, it further reduces to finding

$$\arg\min_{p \in P_b} \sum_{e \in E^* \cap p} \alpha_b^e \quad b \in C^*,$$

which is a weight constrained shortest path problem (WCSPP) defined on the graph $G = (V,E)$ with edge weights $\omega\colon E \to \mathbb{R}_{\geq 0}$, defined as $\omega_e = d_e$, for all $e \in E$ and edge costs $\gamma\colon E \to \mathbb{R}_{\geq 0}$ defined as

$$\gamma_e = \begin{cases} 0, & e \in E^0 \\ \alpha_b^e, & e \in E^* \end{cases} \quad \forall e \in E.$$

Further details regarding pricing will be provided in Section 4.2.

3.3. Cut Formulation

We propose an alternative MILP formulation that is based on a single, *directed communication graph* in which relays are identified by splitting each node i into two copies i_1, i_2. Besides *relay arcs* (i_1, i_2) for each node $i \in V$, we add arcs (j_2, i_1) and (i_2, j_1) for each edge $\{i,j\} \in C$, that is, all incoming arcs target i_1 and all outgoing arcs emanate from i_2. We obtain graph $G'_C = (V'_C, A'_C)$ with node set $V'_C = \{i_1, i_2 \mid i \in V\}$ and arc set $A'_C = \{(i_2,j_1),(j_2,i_1) \mid \{i,j\} \in C\} \cup A_C^r$ where arcs in $A_C^r = \{(i_1,i_2) \mid i \in V\}$ are used to identify relays. An example of a directed communication graph is shown in Figure 7 where solid arcs represent free connections, dotted arcs connections with augmenting edges, and dash-dotted arcs correspond to relays.

The formulation introduced next represents each feasible u,v-walk of a given commodity pair $(u,v) \in \mathcal{K}$

Figure 7. Generation of the Directed Communication Graph $G'_C = (V'_C, A'_C)$ for $d_{\max} = 7$

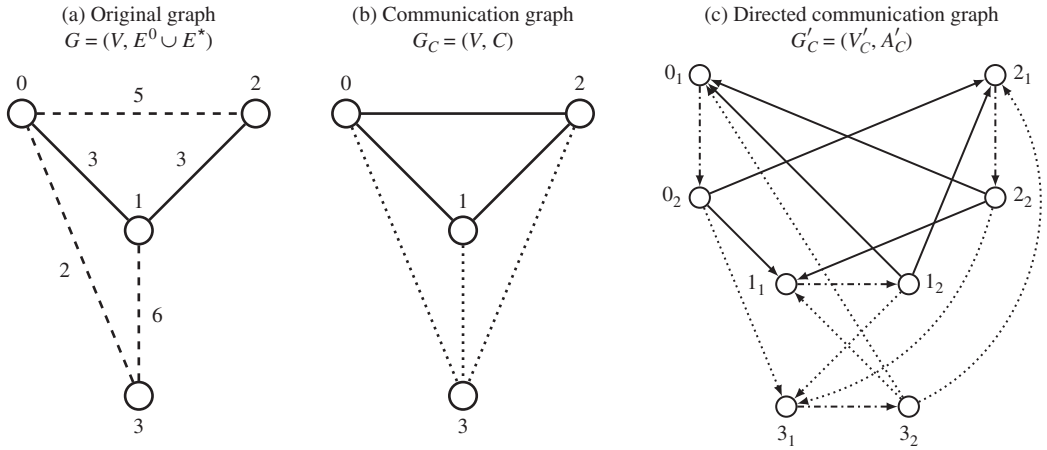

Notes. Nodes are labeled by node index. Edges are labeled by their lengths. Solid lines indicate free edges, dashed lines augmenting edges, and dotted lines indicate connections from C^*. Dash-dotted arcs correspond to relays.

as a directed path from u to v in G'_C with relays placed at all intermediate nodes (cf. Property 3). To this end we utilize binary variables $\mathbf{x}$ for the augmenting edges and path variables $\boldsymbol{\lambda}$, introduced above. In addition, we associate binary variables X_{ij} to the arcs $(i,j) \in A'_C$ of the directed communication graph. Due to the one-to-one correspondence between the arcs in A^r_C and the relays we can use the arc variables directly to identify the relays. The model then reads as follows:

$$\text{(CUT)} \quad \text{minimize} \sum_{i \in V} c_i X_{(i_1,i_2)} + \sum_{e \in E^*} w_e x_e \tag{9}$$

$$\sum_{a \in \delta^-(W)} X_a \geq 1 \quad \forall (u,v) \in \mathcal{K}, \forall W \subset V'_C, v_1 \in W, u_2 \notin W \tag{10}$$

$$-X_{i_2 j_1} + \sum_{p \in P_b} \lambda_b^p \geq 0 \quad \forall b = \{i,j\} \in C^* \quad (\mu_b^1) \tag{11}$$

$$-X_{j_2 i_1} + \sum_{p \in P_b} \lambda_b^p \geq 0 \quad \forall b = \{i,j\} \in C^* \quad (\mu_b^2) \tag{12}$$

$$x_e - \sum_{p \in P_b : e \in p} \lambda_b^p \geq 0 \quad \forall e \in E^*, \forall b \in C^* \quad (\alpha_b^e) \tag{13}$$

$$\lambda_b^p \geq 0 \quad \forall b \in C^*, p \in P_b \tag{14}$$

$$\mathbf{X} \in \{0,1\}^{|A'_C|}, \mathbf{x} \in \{0,1\}^{|E^*|}. \tag{15}$$

We will refer to this model as the *cut formulation on a directed communication graph* (CUT). Cut-set inequalities (10) ensure the existence of a directed path in G'_C from u_2 (the source copy of u) to v_1 (the target copy of v) for each commodity pair $(u,v) \in \mathcal{K}$. By construction, every second arc along this path corresponds to a relay node. Costs for these arcs are included in the objective function. The remaining arcs of type (i_2, j_1) or (j_2, i_1) correspond to paths between i and j, where $b = \{i,j\} \in C^*$. Constraints (11) and (12) ensure that whenever an arc (i_2, j_1) or (j_2, i_1) is used, then at least one corresponding path from $P_{\{i,j\}}$ is selected. Due to the presence of multiple sources, both arcs (i_2, j_1) or (j_2, i_1) can be used in a feasible solution. Finally, constraints (13) ensure that all augmenting edges of the selected paths are included in the solution. Since the number of these constraints is in general exponential, we will separate them dynamically only when violated; see Section 4.3.

Notice that a feasible solution may contain arcs (j_2, i_1) and (i_2, h_1) (for some distinct nodes $i, j, h \in V$), but not necessarily the arc (i_1, i_2). This happens, for example, when node i is both a target and a source, but it is not contained in any connection passing through it (and thus there is no need to install a relay at i). As a consequence, the arcs that correspond to node splitting identify the nodes from V where relays have to be placed, whereas the arcs linking the node copies of i and j map to the paths $p \in P_b$, $b = \{i,j\}$ as in the (MCF) model.

Pricing Subproblem. To formally state the pricing subproblem for variables λ_b^p we associate dual variables $\mu_b^1 \geq 0$ and $\mu_b^2 \geq 0$ to constraints (11) and (12), respectively, and dual variables $\alpha_b^e \geq 0$ to constraints (13). Similar to the previous two cases, for each $b \in C^*$ we need to identify a feasible path with minimum reduced costs

$$\min_{p \in P_b} \left(\sum_{e \in E^* \cap p} \alpha_b^e - \mu_b^1 - \mu_b^2 \right).$$

Thus, we can solve the pricing subproblem by solving for each $b \in C^*$ a WCSPP with edge weights set to α_b^e for $e \in E^*$, and to zero otherwise; see Section 4.2 for more details.

Since formulation (CUT) contains an exponential number of variables ($\boldsymbol{\lambda}$) *and* an exponential number of cut-set constraints (10), a column-and-row generation approach is employed to solve its LP relaxation (and a branch-price-and-cut algorithm to find an optimal solution); see, e.g., Barnhart et al. (1998), Desrosiers

Figure 8. A Partial Solution to the LP Relaxation of (MCF) That Violates Connectivity Constraints (16) for Commodity $(u, v) \in \mathcal{K}$

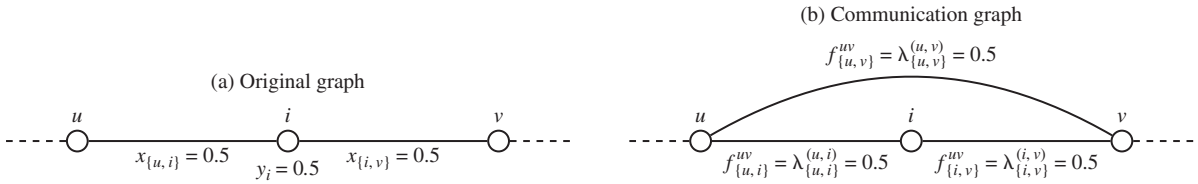

Notes. The total flow in the communication graph from source u to its target v equals 1. However, the minimum u-v cut in the original graph is only 0.5.

and Lübbecke (2011). Fortunately, the λ variables are not involved in the connectivity constraints (10). Thus, we can separate these parts so that column generation can be done independently of cut generation, that is, the added cuts do not influence the structure of the pricing subproblem.

3.4. Valid Inequalities

We now describe several types of valid inequalities that are redundant for the set of feasible solutions but can strengthen the models' LP relaxations.

3.4.1. Connectivity Cuts in the Original Graph. The example given in Figure 8 shows that connectivity constraints (16) can be violated in LP solutions of (MCF) and (CUT), respectively. These constraints ensure that the value of each (undirected) cut separating the source and target of a commodity is at least one. Since cut inequalities including free edges are trivially satisfied, we only consider subsets W inducing cuts without free edges in (16):

$$\sum_{e \in \delta(W)} x_e \geq 1 \quad \forall W \subset V: \delta(W) \cap E^0 = \emptyset, \; \exists (u, v) \in \mathcal{K}: u \notin W, v \in W. \tag{16}$$

One can further strengthen the quality of the LP relaxation by replacing undirected cut-set inequalities (16) by their directed counterparts. To this end, we introduce for each root $u \in \mathcal{K}^S$ variables $z^u_{ij} \geq 0, \forall \{(i, j) | \{i, j\} \in E^*\}$. Variable z^u_{ij} is set to one if one can embed in the original graph a directed path from u to some $v \in \mathcal{K}^T_u$ using arc (i, j). Then, constraints (16) can be enhanced by

$$\sum_{a \in \delta^-(W)} z^u_a \geq 1 \quad \forall W \subset V: \delta(W) \cap E^0 = \emptyset, \; \exists (u, v) \in \mathcal{K}: u \notin W, v \in W \tag{17}$$

$$z^u_{ij} + z^u_{ji} \leq x_{\{i,j\}} \quad \forall u \in \mathcal{K}^S, \{i, j\} \in E^* \tag{18}$$

$$z^u_{ij}, z^u_{ji} \geq 0 \quad \forall u \in \mathcal{K}^S, \{i, j\} \in E^*. \tag{19}$$

It can easily be seen that the directed connectivity constraints (17) are at least as strong as the undirected ones introduced above. From Figure 9 we conclude that they can be strictly stronger if there exists at least one commodity source with more than one target (in the presence of linking constraints (18)). Note that similar to the undirected variant, we do not add cut-set inequalities for node subsets with incident free arcs.

Since both classes of connectivity constraints are of exponential size we will dynamically separate them; see Section 4.3 for details.

3.4.2. Relay Constraints. For the (CUT) model we additionally exploit the fact that a relay has to be placed at some node iff it is an intermediate node along a path within the communication graph. This results in the following constraints that are added to the (CUT) model:

$$\sum_{a \in \delta^-(i_1)} X_a \leq \min(|\mathcal{K}^S|, |\delta(i)| - 1) \cdot X_{(i_1, i_2)} \quad \forall i \notin \mathcal{K}^S \cup \mathcal{K}^T \tag{20}$$

$$\sum_{a \in \delta^+(i_2)} X_a \leq \min(|\mathcal{K}^T|, |\delta(i)| - 1) \cdot X_{(i_1, i_2)} \quad \forall i \notin \mathcal{K}^S. \tag{21}$$

The first set of constraints makes sure that a relay is installed at each node i, which does not belong to any commodity pair, whenever there is an arc entering i_1. Similarly, whenever there is an arc leaving i_2, and node i is not a source, there has to be a relay installed at i.

These constraints benefit from the fact that the (CUT) model uses only one set of variables to ensure connectivity in the communication graph. They are particularly effective if the big-M constants are small, for

Figure 9. A Solution to the LP Relaxation for $\mathcal{K} = \{(u, v_1), (u, v_2)\}$ and $w_{\{u,v_1\}} = w_{\{u,v_2\}} = 1$, $w_{\{v_1,v_2\}} = 3$

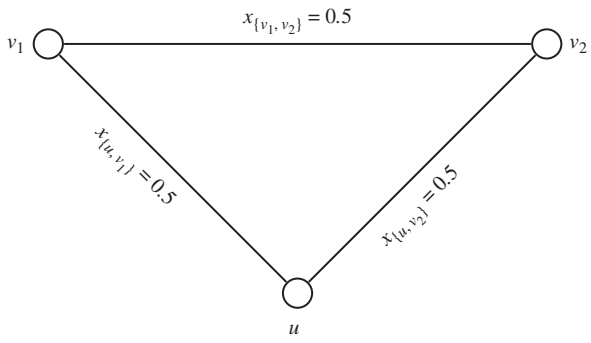

Note. The solution is optimal with respect to the undirected cut-set inequalities but not with respect to the directed ones which will cut off this LP solution.

example, if only a single source node exists. These constraints turned out to be beneficial not only for strengthening the LP relaxation of the (CUT) model, but also for improving the convergence concerning the dynamically separated inequalities.

4. Algorithmic Framework

We developed branch-price-and-cut (BPC) algorithms for the MILP formulations described in the previous section; see Table 1 for a summary. In the following, after providing some remarks on preprocessing that aims to reduce the size of the problem instances, we present additional details (including separation and pricing procedures) of these algorithms.

4.1. Preprocessing

Recall that at the beginning, we remove all edges $e \in E$ such that $d_e > d_{\max}$. If graph G separates into several connected components, and there exists a pair $(u, v) \in \mathcal{H}$ such that u and v belong to different components, then the instance is clearly infeasible. Note that if the problem admits a feasible solution and it contains more than one connected component, every component describes a separate problem instance that can be solved independently. Next, we identify and remove all pairs in $\mathcal{H}$ that can be connected using solely free edges from E^0 and no relays (this can be easily done by applying shortest path algorithms on (V, E^0)).

For the separation procedures explained in Section 4.3, few commodities with many targets per source are preferable. To this end, we use the fact that commodity pairs can be reordered because in an undirected graph the existence of a feasible u, v-walk implies the existence of a feasible v, u-walk. We heuristically reorder the commodities as follows. First, we compute for each node the number of times it appears in a commodity pair. Then, we iteratively choose the node i with the highest count (breaking ties by node index), reorder the commodity pairs involving i by setting i to be the source, and decrease the counts of all nodes by the number of times i is involved in an associated commodity. The procedure is repeated until the count of every node becomes zero.

Table 1. Algorithm Overview

Model	Type B	Graph
(MCF)	BPC $\sum_{(u,v)\in\mathcal{H}} \mu_b^{uv}$	Communication graph G_C
(CUT)	BPC $\mu_b^1 + \mu_b^2$	Directed communication graph G'_C

Note. Name (Model), considered decomposition algorithm (Type), model specific pricing subproblem threshold for WCSPP (B), and considered communication graph (Graph).

4.2. Column Generation

We use column generation to deal with the exponential amount of path variables used in the considered models. The paths we are looking for correspond to the edges of the communication graph. Due to Property 3, these edges correspond to loop-free paths between a pair of nodes i and j, $b = \{i, j\}$. More precisely, for each $b \in C^*$, its reduced costs, denoted by R_b, are calculated as

$$R_b = \min_{p \in P(b)} \sum_{e \in E^* \cap p} \alpha_b^e - B,$$

where the value of the constant B depends on the considered formulation and is given in Table 1.

As already mentioned, for each $b \in C^*$, this pricing subproblem is a WCSPP defined on the graph $G = (V, E)$ with nonnegative edge weights $\omega_e = d_e$, for all $e \in E$ and nonnegative edge costs $\gamma_e = \alpha_b^e$ if $e \in E^*$ and $\gamma_e = 0$, otherwise. The goal is to find a path in G connecting a node pair $b = \{i, j\}$, that minimizes the sum of edge costs and whose weight does not exceed $d_{\max}$.

In our implementation we add one variable corresponding to a least cost path for each $b \in C^*$ in each pricing iteration if it has negative reduced costs. This decision to add at most $|C^*|$ variables in each iteration is based on preliminary experiments indicating that this strategy outperforms other options such as adding only a single variable in each iteration.

Initial Set of Columns. We initially add a set of variables ensuring that there exists a feasible solution to the LP relaxation. To this end, we add a variable corresponding to a connection with minimal length for each $b \in C^*$. Such a connection can easily be found with Dijkstra's algorithm (see Dijkstra 1959) using the edge lengths as costs.

Solving the Pricing Subproblems. The WCSPP on a graph with nonnegative edge costs is a weakly NP-hard problem for which fast pseudo-polynomial exact algorithms are available. For the implementation in our models we use the generic resource-constrained shortest path algorithm from the Boost Graph Library (BGL) in version 1.63.0; see BGL (2016). To speed up performance we prevent path expansions leading to costs larger than or equal to B since such paths can never result in negative reduced costs.

4.3. Separation

Depending on the formulation, up to three different families of exponentially sized constraints can be considered. We separate the three classes in the following order: (i) undirected cut-set inequalities (16) on the original graph; (ii) directed cut-set inequalities (17) on the original graph; and (iii) cut-set inequalities (10) on the communication graph (for the (CUT) model). Only if no violated inequalities of previous classes can be found, we continue with the next class. Violated

inequalities of all three classes are identified by maximum flow computations according to the commodity pairs using the algorithm by Cherkassy and Goldberg (1995). Thereby, the edge (or arc) capacities are set to the current LP solution values plus a small value in order to prefer sparse cuts, that is, those that contain the fewest edges or arcs, respectively. In case of ties, we always choose a cut that is closest to the target node. To avoid adding too many cuts we only consider inequalities that are violated by a value of at least 0.5.

Connectivity in the Original Graph. As noted in Section 3.4.1, directed cuts on the original graph are stronger than their undirected counterpart for commodity sources that need to be considered to more than one target. Therefore, if $|\mathcal{K}_u^{\mathrm{T}}| = 1$ for some $(u, v) \in \mathcal{K}$, we only add undirected cut-set inequalities (16) for this commodity pair. Otherwise, we add variables z^u and consider the directed constraints (17). That way, we always ensure the strongest variant of the connectivity inequalities while avoiding unnecessary overhead whenever possible. We note that such a separation strategy also benefits from the aforementioned reordering of the commodity pairs.

For connectivity cuts based on the original graph, we also consider so-called nested cuts (see, e.g., Ljubić et al. 2006): We set the arc capacities of just added cuts to one and repeat the flow computation to possibly find other violated inequalities. The procedure is continued until no further violations can be detected. Observe that the capacity updates influence the subsequent separation steps. To avoid an unwanted bias we consider the commodity pairs in a random order based on a fixed seed.

Connectivity in the Communication Graph. Since connectivity constraints (10) on the communication graph are not redundant, their separation is not optional, that is, they need to be applied at least to all integer solutions encountered during the branch-and-bound procedure. In our implementation, we additionally use these cuts to cut off fractional solutions, applying the maximum-flow procedures described earlier.

4.4. Initial Pool of Inequalities

We now shortly summarize the set of valid inequalities that are used to initialize our models.

Cuts in the Original Graph. As previously mentioned, both types of the original graph connectivity cuts are dynamically separated. To speed up convergence we add a subset of these inequalities a priori to the model:

$$\sum_{a \in \delta^-(v)} z_a^u = 1 \quad \forall (u, v) \in \mathcal{K}\colon |\mathcal{K}_u^{\mathrm{T}}| > 1, \delta(v) \cap E^0 = \varnothing \tag{22}$$

$$\sum_{a \in \delta^-(i)} z_a^u \le \sum_{a \in \delta^+(i)} z_a^u \quad \forall u \in \mathcal{K}^{\mathrm{S}}\colon |\mathcal{K}_u^{\mathrm{T}}| > 1, \; \forall i \in V \setminus (\mathcal{K}^{\mathrm{S}} \cup \mathcal{K}^{\mathrm{T}}),\ \delta(i) \cap E^0 = \varnothing. \tag{23}$$

If undirected cuts are separated for at least one commodity pair (i.e., $\exists u \in \mathcal{K}^{\mathrm{S}}\colon |\mathcal{K}_u^{\mathrm{T}}| = 1$), we also add the following inequalities since each commodity source and target node has at least one incident edge:

$$\sum_{e \in \delta(i)} x_e \ge 1 \quad \forall i \in V\colon i \in \mathcal{K}^{\mathrm{S}} \cup \mathcal{K}^{\mathrm{T}},\ \delta(i) \cap E^0 = \varnothing. \tag{24}$$

Similarly, we know that relays are never isolated. Thus, we add the following type of inequalities to (MCF):

$$\sum_{e \in \delta(i)} x_e \ge y_i \quad \forall i \in V\colon i \notin \mathcal{K}^{\mathrm{S}} \cup \mathcal{K}^{\mathrm{T}},\ \delta(i) \cap E^0 = \varnothing. \tag{25}$$

Equivalent constraints are considered for the (CUT) model by replacing y_i by $X_{(i_1, i_2)}$.

Cuts in the Communication Graph. We add all constraints from Section 3.4.2 a priori to model (CUT), extended by the following inequalities that ensure that each target has at least one incoming arc and each source has at least one outgoing arc

$$\sum_{a \in \delta^-(v_1)} X_a \ge 1 \quad \forall v \in \mathcal{K}^{\mathrm{T}}$$

$$\sum_{a \in \delta^+(u_2)} X_a \ge 1 \quad \forall u \in \mathcal{K}^{\mathrm{S}}.$$

4.5. Heuristic

Feasible NDPR solutions and initial upper bounds for our algorithms are obtained by using heuristic (CH1) originally introduced in Cabral et al. (2007). Its basic idea is to iteratively compute a solution by solving the problem for the individual commodities. In each iteration all previously added augmenting edges and relays are assigned zero costs. In our implementation we perform 10 runs of (CH1) in which we vary the order in which the commodities are considered (fixed seed random order) and finally adopt the best solution found. Columns required to represent the respective solution are added to the initial formulation.

For each commodity (i.e., in each iteration) we need to solve the minimum cost path problem with relays (MCPPR). Our implementation uses a variant of the pseudo-polynomial dynamic programming algorithm introduced by Laporte and Pascoal (2011). Their algorithm for the MCPPR solves the problem on a directed graph. In the undirected variant we need to make sure that, once an edge has been traversed in one direction, using it in the other direction incurs no additional costs. The simplest way of handling this is to augment the dynamic programming states by a set of already used edges; see Algorithm 4.1 for the adjusted pseudocode. Each state is a tuple of the form $x = (\pi_x^{\mathrm{c}}, \pi_x^{\mathrm{d}}, \xi_x, v_x, E_x^*)$ where π_x^{c} denotes the cost of the current walk, π_x^{d} the distance from the last relay or the starting node along the walk, ξ_x a reference to the preceding state, v_x the final node of the walk, and E_x^* the set of already traversed edges. As suggested in Laporte

and Pascoal (2011), the list of states L is ordered according to nondecreasing cost to allow for early termination once a state containing the target node as final node is reached.

Algorithm 4.1 (Dynamic programming algorithm for the minimum connected path problem with relays in an undirected graph)

Input: Graph $G = (V, E, c, w, d)$, $E = E^0 \cup E^*$, pair $(s, t) \in \mathcal{K}$
Data: M_{di} ... cheapest path to i at distance d, L ... set of unexpanded states

$L \leftarrow \{(0, 0, NULL, s, \emptyset)\}$
forall $d \in \{0, \dots, d_{\max}\}$, $i \in V$ **do** $M_{di} \leftarrow NULL$
while $L \neq \emptyset$ **do**
  select first $x \in L$ and remove it from L
  forall $\{v_x, j\} \in \delta(v_x)$ **do**
    $\hat{d} \leftarrow \pi^{\mathrm{d}}_x + d_{\{v_x, j\}}$ // arrival distance at j
    if $\hat{d} \le d_{\max}$ **then**
      $\hat{c} \leftarrow \pi^{\mathrm{c}}_x$ // cost at j
      if $\{v_x, j\} \notin E^0 \cup E^*_x$ **then** $\hat{c} \leftarrow \hat{c} + w_{\{v_x, j\}}$
      $\hat{E}^* \leftarrow E^*_x \cup (\{v_x, j\} \cap E^*)$ // traversed augmenting edges at j
      if $j \neq t \wedge (M_{0j} = NULL \vee \hat{c} + c_j < \pi^{\mathrm{c}}_{M_{0j}})$ **then** // expansion with relay at j
        $M_{0j} \leftarrow (\hat{c} + c_j, 0, x, j, \hat{E}^*)$
        $L \leftarrow L \cup \{M_{0j}\}$
      if $M_{\hat{d}j} = NULL \vee \hat{c} < \pi^{\mathrm{c}}_{M_{\hat{d}j}}$ **then** // expansion without relay at j
        $M_{\hat{d}j} \leftarrow (\hat{c}, \hat{d}, x, j, \hat{E}^*)$
        $L \leftarrow L \cup \{M_{\hat{d}j}\}$
return $\arg\min_{x \in M_{dt}: 0 \le d \le d_{\max}} \pi^{\mathrm{c}}_x$

After the 10 runs of (CH1) we perform a final run for which we set the costs of all relays and edges selected by the best solution to zero. The idea behind this run is to remove possible redundancies with respect to the selected relays and edges. Thereby, it is important to break ties regarding the ordering of L by prioritizing states with smaller π^{d}_x. We denote the modified algorithm by (CH1+).

4.6. Solver Configuration

Our algorithms are implemented in C++ using SCIP 3.2.1 (see Gamrath et al. 2016) as branch-price-and-cut framework and CPLEX 12.6.3 as LP solver. The dual simplex method has been used for solving the LP relaxations as it outperformed other options (primal simplex, barrier) in preliminary experiments. All experiments have been performed in single thread mode with presolving, probing, and the solvers general purpose heuristics turned on. General purpose cutting planes have been deactivated.

5. Computational Study

In this section we first give details on benchmark instances, which are then used to compare the performance of the developed branch-price-and-cut algorithms and to demonstrate their advantages and drawbacks.

5.1. Benchmark Instances

We consider three groups of benchmark instances: (1) instances from Cabral et al. (2007), (2) instances introduced by Konak (2012), and (3) an entirely new set of instances (ARLP), generated to reflect some of the real-world properties not covered by the previous two families.

Cabral Instances. These instances have been introduced by Cabral et al. (2007); see Table 2 for an overview. They are extremely sparse four-grid graphs in which each node is connected only to its direct vertical and horizontal neighbors. All edges have costs greater than zero (i.e., $E^0 = \emptyset$) and the maximum distance is equal to 70 for all instances. There are 180 instances in this family: for a fixed input graph and the given number of commodities, 10 instances are generated by sampling the set of commodities. All commodities share one node, that is, we can reorder them such that $|\mathcal{K}^{\mathrm{S}}| = 1$. The number of nodes varies between 20 and 60. Although $|\mathcal{K}| \in \{5, 10\}$, we point out that for some instances the "effective" number of commodities is smaller than specified by the instance. This is because of two reasons: First, some instances contain the same commodity more than once. Second, some instances contain commodities for which the source and target are identical. Since commodities of this type are trivially connected by the empty path, we simply ignore them. Column $|\mathcal{K}|$ in Table 2 reports the average number of effective commodity pairs.

Konak Instances. These instances that were generated by randomly placing and connecting nodes on a grid were originally introduced by Konak (2012). The number of nodes varies between 40 and 160. The length of each edge $\{i, j\}$ is set to the Euclidean distance between i and j while its cost is either set equal to the edge length (type I) or to $d_{\max} - d_{\{i,j\}}$ (type II). The basic instance properties ($|V|$, $|E^0|$, $|E^*|$, $|\mathcal{K}|$, and $d_{\max}$) are shown in Tables 3 and 4. Instances with an identical number of nodes and the same $d_{\max}$ are based on the same graph and only the number of commodities differs. There are 40 instances in total, 20 of each type. Notice that also for this family of instances, the number of commodities is extremely low ($|\mathcal{K}| \in \{5, 10\}$). In some instances free edges are present but their number is always rather small.

ARLP Instances. This newly generated set of benchmark instances is intended to complement the previous two sets available from the literature. Both Cabral and

Table 2. Results on the Cabral Instances

					LP		IP					
					Gap [%]		Opt. gap [%]		t [s]		Columns	
Instance	$\|V\|$	$\|E^*\|$	$\|\mathcal{K}\|$	(CH1+)	(MCF)	(CUT)	(MCF)	(CUT)	(MCF)	(CUT)	(MCF)	(CUT)
4A5B70L5K	20	31	4.5	100.2	**0.7**	**0.7**	**0.0**	**0.0**	**<1**	**<1**	**21**	24
4A5B70L10K	20	31	7.9	103.8	1.4	**1.2**	**0.0**	**0.0**	**1**	**1**	**34**	51
5A5B70L5K	25	40	4.2	105.0	1.6	**1.4**	**0.0**	**0.0**	1	**<1**	**34**	39
5A5B70L10K	25	40	8.5	105.7	1.6	**1.5**	**0.0**	**0.0**	**1**	**1**	**49**	70
6A5B70L5K	30	49	4.7	101.3	0.6	**0.2**	**0.0**	**0.0**	**1**	**1**	**48**	50
6A5B70L10K	30	49	8.8	102.1	2.0	**1.5**	**0.0**	**0.0**	4	**3**	**78**	102
7A5B70L5K	35	58	4.5	101.6	1.4	**1.2**	**0.0**	**0.0**	**1**	2	57	**50**
7A5B70L10K	35	58	8.4	102.3	2.1	**1.7**	**0.0**	**0.0**	6	**5**	**98**	115
8A5B70L5K	40	67	4.7	103.3	1.6	**1.2**	**0.0**	**0.0**	4	**3**	90	**73**
8A5B70L10K	40	67	8.9	106.0	2.9	**2.6**	**0.0**	**0.0**	11	**7**	**127**	142
9A5B70L5K	45	76	4.8	105.3	**1.3**	**1.3**	**0.0**	**0.0**	4	**2**	88	**66**
9A5B70L10K	45	76	9.0	105.3	2.4	**1.9**	**0.0**	**0.0**	19	**8**	176	**158**
10A5B70L5K	50	85	5.0	103.5	2.2	**1.6**	**0.0**	**0.0**	8	**7**	127	**111**
10A5B70L10K	50	85	9.4	104.3	2.4	**2.3**	**0.0**	**0.0**	32	**14**	210	**184**
11A5B70L5K	55	94	4.6	100.8	1.9	**1.8**	**0.0**	**0.0**	5	**4**	103	**86**
11A5B70L10K	55	94	9.1	105.7	1.3	**0.4**	**0.0**	**0.0**	45	**11**	242	**170**
12A5B70L5K	60	103	4.7	104.7	1.2	**0.8**	**0.0**	**0.0**	9	**8**	142	**114**
12A5B70L10K	60	103	9.0	103.0	3.9	**2.6**	**0.0**	**0.0**	179	**26**	357	**252**

Notes. Column $|\mathcal{K}|$ reports the average number of effective commodity pairs. (CH1+) gives the ratio between the objective value obtained by the heuristic and the best-known upper bound. We report the LP gap, the optimality gap, the total computing time in seconds (t [s]), and the number of priced columns. Each row reports a mean value over a set of 10 instances. Best values are marked bold.

Konak instances assume $|\mathcal{K}| \in \{5, 10\}$. On the contrary, ARLP instances aim to simulate applications where many node pairs needs to communicate. We refer to this set as augmented RLP (ARLP) instances since we require all nodes to communicate with each other, as it is the case for the RLP (cf. Section 1.2). In contrast to

Table 3. Results on the Konak Instances (Type I)

								LP		IP					
								Gap [%]		Opt. gap [%]		t [s]		Columns	
Instance	$\|V\|$	$\|E^0\|$	$\|E^*\|$	$\|\mathcal{K}\|$	$d_{\max}$	UB^*	(CH1+)	(MCF)	(CUT)	(MCF)	(CUT)	(MCF)	(CUT)	(MCF)	(CUT)
40N_5K_30L	40	0	198	5	30	**473.80**	102.7	**11.9**	**11.9**	**0.0**	**0.0**	**16**	27	299	**227**
40N_5K_35L	40	0	272	5	35	**352.08**	102.7	**21.0**	**21.0**	**0.0**	**0.0**	1,173	**533**	1,012	**767**
40N_10K_30L	40	0	198	10	30	**518.98**	108.2	**15.9**	**15.9**	**0.0**	**0.0**	180	**152**	**401**	421
40N_10K_35L	40	0	272	10	35	399.36	112.3	**23.1**	**23.1**	**6.6**	8.0	7,200	7,200	1,043	**1,027**
50N_5K_30L	50	0	279	5	30	**283.79**	120.3	**0.0**	**0.0**	**0.0**	**0.0**	**1**	5	232	**186**
50N_5K_35L	50	0	372	5	35	**260.24**	100.0	**1.2**	**1.2**	**0.0**	**0.0**	**6**	27	565	**499**
50N_10K_30L	50	0	279	10	30	**540.39**	103.8	**13.0**	**13.0**	**0.0**	**0.0**	**158**	411	**540**	557
50N_10K_35L	50	0	372	10	35	**404.32**	111.9	**11.8**	**11.8**	**0.0**	**0.0**	**204**	261	**1,177**	1,307
60N_5K_30L	60	0	305	5	30	**509.12**	103.2	**21.5**	**21.5**	**0.0**	**0.0**	**39**	70	**509**	541
60N_5K_35L	60	0	412	5	35	**377.02**	105.8	**10.9**	**10.9**	**0.0**	**0.0**	**48**	94	**939**	1,146
60N_10K_30L	60	0	305	10	30	**678.84**	107.0	**24.4**	**24.4**	**0.0**	**0.0**	**886**	1,063	**703**	730
60N_10K_35L	60	0	412	10	35	**499.64**	112.9	**19.0**	**19.0**	**0.0**	**0.0**	**891**	1,400	**1,498**	1,520
80N_5K_30L	80	0	641	5	30	353.86	105.2	**15.7**	**15.7**	**9.1**	10.0	7,200	7,200	3,887	**3,784**
80N_5K_35L	80	0	853	5	35	334.21	103.2	**19.9**	TL	**16.1**	16.7	7,200	7,200	9,110	**8,394**
80N_10K_30L	80	0	641	10	30	513.02	100.0	**36.7**	TL	**32.0**	35.2	7,200	7,200	**3,613**	3,815
80N_10K_35L	80	0	853	10	35	516.91	100.0	**43.0**	TL	44.4	**42.2**	7,200	7,200	**6,952**	8,592
160N_5K_30L	160	3	2,770	5	30	298.31	100.0	**29.7**	TL	29.6	**28.2**	7,200	7,200	**15,941**	23,489
160N_5K_35L	160	3	3,621	5	35	314.52	100.0	TL	**37.0**	58.1	**37.2**	7,200	7,200	**20,303**	30,877
160N_10K_30L	160	3	2,770	10	30	470.54	100.0	TL	TL	TL	**44.1**	7,200	7,200	**11,229**	23,027
160N_10K_35L	160	3	3,621	10	35	484.97	100.0	TL	TL	TL	**50.2**	7,200	7,200	**11,872**	36,042

Notes. Column UB^* provides the best-known upper bounds, optimal bounds are marked bold. (CH1+) gives the ratio between the objective value obtained by the heuristic and the best-known upper bound. We report the LP gap, the optimality gap, the total computing time in seconds (t [s]), and the number of priced columns. Best values are marked bold. If an algorithm failed to compute a lower bound due to the time limit, the respective gap entry is marked with "TL."

Table 4. Results on the Konak Instances (Type II)

								LP		IP					
								Gap [%]		Opt. gap [%]		t [s]		Columns	
Instance	$\|V\|$	$\|E^0\|$	$\|E^*\|$	$\|\mathcal{K}\|$	$d_{\max}$	UB^*	(CH1+)	(MCF)	(CUT)	(MCF)	(CUT)	(MCF)	(CUT)	(MCF)	(CUT)
40N_5K_30L	40	1	197	5	30	**247.27**	100.1	**0.0**	**0.0**	**0.0**	**0.0**	**<1**	1	111	**80**
40N_5K_35L	40	0	272	5	35	**111.30**	101.7	**7.1**	**7.1**	**0.0**	**0.0**	**9**	17	459	**314**
40N_10K_30L	40	1	197	10	30	**292.62**	100.1	**4.4**	**4.4**	**0.0**	**0.0**	**13**	18	293	**267**
40N_10K_35L	40	0	272	10	35	**140.51**	101.0	**7.7**	**7.7**	**0.0**	**0.0**	61	**45**	690	**625**
50N_5K_30L	50	1	278	5	30	**119.80**	100.0	**0.0**	**0.0**	**0.0**	**0.0**	**<1**	1	**98**	104
50N_5K_35L	50	0	372	5	35	**155.57**	105.2	**1.0**	**1.0**	**0.0**	**0.0**	**2**	33	**422**	547
50N_10K_30L	50	1	278	10	30	**279.70**	100.6	**2.0**	TL	**0.0**	**0.0**	**3**	28	**247**	432
50N_10K_35L	50	0	372	10	35	**206.22**	102.1	**1.6**	TL	**0.0**	**0.0**	**32**	127	**828**	1,303
60N_5K_30L	60	3	302	5	30	**317.32**	104.0	**14.2**	**14.2**	**0.0**	**0.0**	**7**	26	**337**	444
60N_5K_35L	60	0	412	5	35	**166.35**	100.0	**0.0**	**0.0**	**0.0**	**0.0**	**<1**	3	**315**	446
60N_10K_30L	60	3	302	10	30	**414.32**	120.4	**12.2**	**12.2**	**0.0**	**0.0**	**52**	88	**444**	583
60N_10K_35L	60	0	412	10	35	**242.32**	100.1	**5.2**	**5.2**	**0.0**	**0.0**	**21**	53	**748**	1,016
80N_5K_30L	80	2	639	5	30	**134.73**	108.6	**4.9**	**4.9**	**0.0**	**0.0**	**32**	167	**1,455**	1,705
80N_5K_35L	80	1	852	5	35	**104.04**	100.4	**2.0**	**2.0**	**0.0**	**0.0**	**46**	306	**2,307**	2,899
80N_10K_30L	80	2	639	10	30	**187.17**	105.0	**8.1**	**8.1**	**0.0**	**0.0**	695	**625**	2,756	**2,501**
80N_10K_35L	80	1	852	10	35	**168.62**	102.2	**11.2**	TL	**0.0**	12.9	**4,382**	7,200	**7,947**	9,114
160N_5K_30L	160	9	2,764	5	30	**78.61**	106.2	**6.6**	**6.6**	**0.0**	4.2	**1,491**	7,200	**12,812**	23,985
160N_5K_35L	160	9	3,615	5	35	**68.15**	101.4	**9.0**	**9.0**	**0.0**	6.7	**5,273**	7,200	**29,676**	30,003
160N_10K_30L	160	9	2,764	10	30	112.06	106.1	**6.5**	TL	**5.7**	11.6	7,200	7,200	**16,850**	26,344
160N_10K_35L	160	9	3,615	10	35	117.19	100.0	TL	TL	**10.3**	33.4	7,200	7,200	**22,324**	34,909

Notes. Column UB^* provides the best-known upper bounds, optimal bounds are marked bold. (CH1+) gives the ratio between the objective value obtained by the heuristic and the best-known upper bound. We report the LP gap, the optimality gap, the total computing time in seconds (t [s]), and the number of priced columns. Best values are marked bold. If an algorithm failed to compute a lower bound due to the time limit, the respective gap entry is marked with "TL."

the RLP, the set of augmenting edges E^* is not empty, and in contrast to the Konak and Cabral instances, a significant number of zero cost edges exists.

The instances have been generated as follows. Nodes are placed randomly on a 100×100 grid and edges with length equal to the Euclidean distance (rounded up) between two nodes are added whenever this distance does not exceed 30. Each edge is chosen to be a free edge with probability 20%, 50%, or 80% in instance subsets `20F`, `50F`, and `80F`, respectively. The costs w_{ij} of augmenting edges $\{i, j\}$ are chosen randomly according to a normal distribution with parameters $\mu = d_{ij}, \sigma = 5$ (rounded up). Relay costs are chosen randomly according to the normal distribution $\mu = 10 \cdot \bar{w}, \sigma = 20$ (rounded up) where $\bar{w}$ denotes the average costs of augmenting edges. Finally, $d_{\max} = 50$ for all instances and $\mathcal{K}$ contains all pairs that cannot be connected using solely free edges, that is, $\mathcal{K} = \{(u, v) \mid (u, v) \in V \times V, u < v\} \backslash C^0$ (see Section 4.1).

In addition, a second set of instances (denoted as ARLP-p25) with a smaller number of commodities has been created. Each such instance is generated from an ARLP instance by adopting each commodity with a probability of 25%. The main characteristics of sets ARLP and ARLP-p25 are summarized in Tables 5 and 6, respectively. The instances are already preprocessed, in the sense that our preprocessing procedures do not apply. Especially, we only consider instances that are connected, that is, they consist of a single connected component. Furthermore, we define the set $\mathcal{K}$ so that commodity pairs that can be connected only using free edges and without relays are not included.

The ARLP and the ARLP-p25 instance sets are available at https://www.ac.tuwien.ac.at/research/problem-instances/#Network_Design_Problem_with_Relays.

5.2. Computational Results

Test results reported in this section have been obtained on an Intel Xeon E5540 machine with 2.53 GHz. The computing time limit has been set to 7,200 seconds and the memory limit to 8 GB RAM. As discussed in Section 4.3 we use a violation threshold of 0.5 when separating strengthening inequalities. This threshold is only considered when solving the problem to integer optimality. When reporting LP bounds in this section, we add all violated inequalities. This means that independent experiments are conducted for the two cases. This leads to situations in which the integer run finds an optimal solution but the LP run terminates due to the time or the memory limit as a result of excessive separation of cutting planes. Conversely, it is also possible that the LP gap is tighter than the final optimality gap of the integer run if the latter cannot progress fast enough.

Table 5. Results on the ARLP Instances

							LP		IP					
							Gap [%]		Opt. gap [%]		t [s]		Columns	
Instance	$\|V\|$	$\|E^0\|$	$\|E^*\|$	$\|\mathcal{K}\|$	UB^*	(CH1+)	(MCF)	(CUT)	(MCF)	(CUT)	(MCF)	(CUT)	(MCF)	(CUT)
40N50L20F_A	40	26	124	724	**874**	122.5	TL	**10.7**	TL	**0.0**	7,200	**142**	**132**	1,340
40N50L20F_B	40	35	123	688	**874**	113.3	TL	**13.4**	TL	**0.0**	7,200	**139**	**147**	1,196
40N50L50F_A	40	89	78	513	**837**	103.9	**15.2**	**15.2**	**0.0**	**0.0**	2,504	**14**	**59**	83
40N50L50F_B	40	71	72	586	**876**	108.3	**6.4**	**6.4**	**0.0**	**0.0**	2,683	**7**	76	**74**
40N50L80F_A	40	146	32	443	**516**	100.0	**0.0**	**0.0**	**0.0**	**0.0**	10	**2**	1	**0**
40N50L80F_B	40	154	35	423	**777**	100.9	**6.6**	**6.6**	**0.0**	**0.0**	155	**5**	**18**	23
50N50L20F_A	50	44	212	1,111	**815**	106.5	TL	**5.9**	ML	**0.0**	ML	**416**	ML	**3,973**
50N50L20F_B	50	59	235	1,022	**656**	131.2	TL	**2.8**	ML	**0.0**	ML	**72**	ML	**3,032**
50N50L50F_A	50	132	157	719	**543**	104.4	**9.6**	TL	ML	**0.0**	ML	**11**	ML	**114**
50N50L50F_B	50	117	132	873	**775**	100.8	TL	**5.8**	ML	**0.0**	ML	**30**	ML	**211**
50N50L80F_A	50	175	51	788	**630**	143.8	**11.1**	TL	**0.0**	**0.0**	211	**10**	25	**7**
50N50L80F_B	50	212	58	682	**572**	119.2	**0.0**	**0.0**	**0.0**	**0.0**	29	**5**	1	**0**
60N50L20F_A	60	72	269	1,549	**775**	111.1	ML	**5.5**	ML	**0.0**	ML	**257**	ML	**3,685**
60N50L20F_B	60	63	268	1,588	**976**	129.7	ML	**17.8**	ML	**0.0**	ML	**1,397**	ML	**3,725**
60N50L50F_A	60	216	204	1,036	**628**	115.8	TL	ML	ML	**0.0**	ML	**44**	ML	**201**
60N50L50F_B	60	197	200	1,103	**743**	103.0	TL	ML	ML	**0.0**	ML	**58**	ML	**255**
60N50L80F_A	60	311	85	854	**503**	119.7	**2.1**	TL	ML	**0.0**	ML	**16**	ML	**16**
60N50L80F_B	60	283	74	1,041	**624**	110.1	**9.9**	ML	ML	**0.0**	ML	**18**	ML	**4**
80N50L20F_A	80	123	525	2,729	1,084	100.0	ML	**35.1**	ML	**34.0**	ML	7,200	ML	**19,111**
80N50L20F_B	80	124	545	2,659	790	125.8	ML	TL	ML	**9.6**	ML	7,200	ML	**21,190**
80N50L50F_A	80	335	342	1,916	**498**	120.9	ML	ML	ML	**0.0**	ML	**65**	ML	**71**
80N50L50F_B	80	366	375	1,902	**541**	135.5	ML	TL	ML	**0.0**	ML	**159**	ML	**424**
80N50L80F_A	80	548	148	1,834	**577**	101.4	ML	ML	ML	**0.0**	ML	**67**	ML	**5**
80N50L80F_B	80	597	158	1,532	**549**	159.2	ML	ML	ML	**0.0**	ML	**85**	ML	**4**

Notes. Column UB^* provides the best-known upper bounds, optimal bounds are marked bold. (CH1+) gives the ratio between the objective value obtained by the heuristic and the best-known upper bound. We report the LP gap, the optimality gap, the total computing time in seconds (t [s]), and the number of priced columns. Best values are marked bold. Entries marked with "ML" indicate that an experiment has been terminated because of the memory limit. If an algorithm failed to compute a lower bound because of the time limit, the respective gap entry is marked with "TL."

Tables 2–6 summarize the results. Both models (MCF) and (CUT) are compared with respect to the LP relaxation gap (LP Gap [%]), the final optimality gap (Opt. Gap [%]), the used computing time (t [s]), and the number of priced columns (Columns). LP and optimality gaps are computed as $100 \cdot ((UB^* - LB)/UB^*)$ where UB^* is the best-known upper bound and LB is the lower bound obtained by the respective algorithm. The upper bounds shown in the tables in the column UB^* are printed bold iff the given value is shown to be the optimal objective value by any of the considered algorithms. Entries marked with "ML" indicate that an experiment has been terminated because of the memory limit. Furthermore, for some of the most challenging instances it was impossible to obtain a lower bound within the imposed time limit. In these cases the LP or optimality gap cannot be computed and respective fields are marked with "TL." Finally, for the heuristic (CH1+) we report the percentage increase with respect to the best-known upper bound given by $100 \cdot (UB^H/UB^*)$ where UB^H is the objective value obtained by (CH1+).

5.2.1. Cabral Instances. Mean values of the computational results obtained for instances from set Cabral are provided in Table 2. Each row corresponds to 10 instances for the given instance graph and the number of commodities.

We first notice that both algorithms provide very small LP gaps, with the gaps from (CUT) being consistently smaller than those from (MCF). This can be explained by the fact that the big-M coefficients in inequalities (20) are equal to one since all commodities have the same source in this instance set. This advantage concerning the quality of LP bounds carries over to the integral runs leading to significantly smaller computing times for the (CUT) model. Both models require a comparable number of columns to solve the instances to optimality. In general, the number of priced columns is rather low, which can be explained by the sparsity of the considered input graphs.

Our results constitute a clear improvement compared to the results reported by Cabral et al. (2007) where these instances have been introduced. Whereas Cabral et al. (2007) provide only heuristic solutions with relatively large optimality gaps (with up to 20% with respect to their best-performing arc-path based formulation), we are able to solve all instances to provable optimality—in most cases within a few seconds

Table 6. Results on the ARLP-p25 Instances

							LP		IP					
							Gap [%]		Opt. gap [%]		t [s]		Columns	
Instance	$\|V\|$	$\|E^0\|$	$\|E^*\|$	$\|\mathcal{K}\|$	UB^*	(CH1+)	(MCF)	(CUT)	(MCF)	(CUT)	(MCF)	(CUT)	(MCF)	(CUT)
40N50L20F_A_p25	40	26	124	181	**874**	119.2	**11.4**	**11.4**	11.7	**0.0**	7,200	**106**	**499**	1,429
40N50L20F_B_p25	40	35	123	172	**874**	102.7	**14.6**	**14.6**	11.2	**0.0**	7,200	**109**	**529**	1,238
40N50L50F_A_p25	40	89	78	129	**837**	102.2	**15.2**	**15.2**	**0.0**	**0.0**	152	**10**	**58**	81
40N50L50F_B_p25	40	71	72	147	**876**	104.8	**6.4**	**6.4**	**0.0**	**0.0**	112	**3**	**80**	96
40N50L80F_A_p25	40	146	32	111	**516**	100.0	**0.0**	**0.0**	**0.0**	**0.0**	2	**1**	2	**0**
40N50L80F_B_p25	40	154	35	106	**777**	100.9	**6.6**	**6.6**	**0.0**	**0.0**	20	**2**	**16**	22
50N50L20F_A_p25	50	44	212	278	**815**	106.0	TL	**6.1**	TL	**0.0**	7,200	**611**	**572**	4,396
50N50L20F_B_p25	50	59	235	256	**656**	122.0	TL	**2.8**	TL	**0.0**	7,200	**209**	**547**	4,256
50N50L50F_A_p25	50	132	157	180	**543**	112.0	**9.6**	**9.6**	**0.0**	**0.0**	179	**5**	**142**	153
50N50L50F_B_p25	50	117	132	219	**775**	100.0	**5.8**	**5.8**	**0.0**	**0.0**	4,431	**11**	273	**184**
50N50L80F_A_p25	50	175	51	197	**630**	124.0	**11.1**	**11.1**	**0.0**	**0.0**	26	**2**	17	**3**
50N50L80F_B_p25	50	212	58	171	**572**	119.2	**0.0**	**0.0**	**0.0**	**0.0**	6	**1**	**1**	3
60N50L20F_A_p25	60	72	269	388	**775**	116.3	TL	**5.5**	TL	**0.0**	7,200	**2,174**	**366**	4,904
60N50L20F_B_p25	60	63	268	397	**976**	126.0	TL	**18.4**	TL	**0.0**	7,200	**4,412**	**343**	4,037
60N50L50F_A_p25	60	216	204	259	**628**	115.8	**8.0**	TL	**0.0**	**0.0**	6,777	**46**	**220**	237
60N50L50F_B_p25	60	197	200	276	**743**	122.3	**8.5**	**8.5**	4.7	**0.0**	7,200	**45**	**242**	360
60N50L80F_A_p25	60	311	85	214	**503**	148.7	**2.1**	**2.1**	**0.0**	**0.0**	125	**7**	25	**24**
60N50L80F_B_p25	60	283	74	261	**624**	124.5	**9.9**	**9.9**	**0.0**	**0.0**	81	**16**	15	**14**
80N50L20F_A_p25	80	123	525	683	1,095	100.0	TL	**35.8**	ML	**33.9**	ML	7,200	ML	**19,296**
80N50L20F_B_p25	80	124	545	665	1,024	100.0	TL	TL	ML	**35.4**	ML	7,200	ML	**21,959**
80N50L50F_A_p25	80	335	342	479	**498**	120.9	**1.1**	TL	**0.0**	**0.0**	1,890	**28**	**155**	193
80N50L50F_B_p25	80	366	375	476	**541**	141.6	TL	TL	TL	**0.0**	7,200	**181**	**224**	538
80N50L80F_A_p25	80	548	148	459	**577**	100.2	**2.6**	TL	**0.0**	**0.0**	826	**40**	17	**14**
80N50L80F_B_p25	80	597	158	383	**549**	132.1	**9.7**	TL	**0.0**	**0.0**	1,580	**55**	13	**12**

Notes. Column UB^* provides the best-known upper bounds, optimal bounds are marked bold. (CH1+) gives the ratio between the objective value obtained by the heuristic and the best-known upper bound. We report the LP gap, the optimality gap, the total computing time in seconds (t [s]), and the number of priced columns. Best values are marked bold. Entries marked with "ML" indicate that an experiment has been terminated because of the memory limit. If an algorithm failed to compute a lower bound because of the time limit, the respective gap entry is marked with "TL."

only. Moreover, our (CUT) formulation features very small LP gaps that range between 0.2% and 2.6% on these instances.

5.2.2. Konak Instances. In contrast to the Cabral instances, for this data set, the number of targets per given source does not exceed two (and is usually only one). Hence, the structure of optimal solutions on the communication graph is less arborescence like, it is rather an intersection of multiple source-target walks. In Tables 3 and 4 we compare the performance of the proposed exact approaches for instances of type I and type II, respectively. We report the LP gaps, the final optimality gaps, the overall computing times, and the numbers of priced columns. Among the instances of type I and II, 11 of 20 and 18 of 20 are solved to optimality, respectively. Interestingly, it turns out that instances with edge lengths equivalent to the costs (type I) are significantly harder to solve for our algorithms than those where edge costs and edge lengths are inversely correlated (type II).

***Konak Type* I.** We first compare the LP gaps reported in Table 3. Considering only those cases when both algorithms are able to finish the computation of the LP bound, we observe that the gaps of both formulations are the same. This is not surprising since the benefits of inequalities (20) diminish due to multiple source and target nodes in each instance. In general, these instances are much harder to solve for our algorithms than those from the Cabral set. The main reason is that the graphs are much denser, which leads to higher separation and pricing efforts.

The performance for the complete runs (until finding an optimal integer solution or reaching the time limit) is consistent with the LP bound results. While the majority of instances with at most 60 nodes could be solved by both algorithms, the final optimality gaps are quite large for instances with 80 and more nodes. Both algorithms feature similar computing times with a slight advantage for the (MCF) model. The main advantage of the (CUT) formulation is that it can provide bounds for all instances. The (MCF), on the other hand, cannot provide bounds for the two most difficult instances within the time limit of two hours. We observe that our algorithms improve the initial upper bounds received from the heuristic (reported in the column (CH1+)) for all but two instances with 80 nodes and the instances with 160 nodes.

***Konak Type* II.** The results shown in Table 4, compared with those obtained for instances of type I, clearly indicate that for our algorithms type II instances are easier to solve than the type I instances. The above discussed relation between the two approaches remains roughly the same, both regarding the quality of the LP gaps and the overall performance. In total, 18 of 20 instances of this group could be solved to optimality by the (MCF), three more than by the (CUT) model. The LP gaps are much smaller than for the type I instances and for two instances the LP gap is even zero. The upper bounds obtained from (CH1+) have been shown to be optimal by our algorithms in two cases and have been improved by them for all remaining ones except the largest one (`160N_10K_35L`).

5.2.3. ARLP Instances. Recall that the Cabral and Konak instances contain very few commodities and almost no free edges. The influence of the ratio of free edges to augmenting edges on the proposed approaches as well as the influence of a larger number of commodities is therefore investigated on the set of ARLP instances. Results obtained for the ARLP instances and all considered percentages of free edges (20%, 50%, or 80% of all available edges) are provided in Table 5. It is not surprising that the most difficult instances are those with only 20% free edges and that the instances become significantly easier to solve with an increasing number of free edges. Notice that, because of the huge number of commodities, the model (MCF), which performed quite well on the other two data sets, can now only deal with the smallest instances with 40 nodes and some instances with 50 nodes. For larger instances, (MCF) always hits the memory limit, because of its excessive size. Clearly, using the (CUT) model greatly helps to overcome this issue.

As before, (MCF) provides the same LP gaps as (CUT) whenever both models manage to terminate within the time limit. The ARLP instances are more challenging for the (CUT) model as well. This can be explained by the excessive number of cuts that need to be generated, especially for the calculation of LP bounds, where no violation threshold is used. Moreover, the effects of the connectivity cuts in the original graph diminish on this data set, due to the presence of a substantial number of free edges. Overall, (CUT) is clearly the best-performing model for this data set. It is able to find optimal solutions for 22 of 24 instances. The (MCF) model, on the other hand, manages to solve only six instances to optimality. As for the other instance sets, the upper bounds obtained from (CH1+) are improved for almost all instances by our algorithms, which only fail to improve them for one of the most challenging problems (`80N50L20F_A`) and prove optimality of one solution obtained by (CH1+).

ARLP-p25 instances. The purpose of evaluating our algorithms on this family of instances was to study the influence of the number of commodities to the algorithmic performance. Recall that for the ARLP instances, each node pair is a commodity, that is, $|\mathcal{K}|$ is in $O(|V|^2)$. For the ARLP-p25 instances, the number of commodities is reduced to a quarter. In general, the results indicate that as long as the number of commodities remains $O(|V|^2)$, the NDPR is much more difficult to solve than when the number of commodities is fixed to a small constant value (as this was the case for the Cabral and the Konak instances). Moreover, the remaining commodities still enforce solutions that guarantee full connectivity since the optimal objective values do not change for the corresponding instances. The detailed results are provided in Table 6.

Again, the LP gaps of both models are the same whenever both of them terminated within the time limit. However, this time more LP bounds have been obtained because of the smaller number of commodities. The quality of the bounds is roughly comparable to those of the ARLP instances. The number of optimal solutions found does not change when reducing the number of commodities, that is, optimal solutions have been found for 22 out of 24 instances. For the (MCF) the number of instances solved to optimality greatly increases from 6 to 14, mainly because of the smaller number of commodities reducing the size of the model. Surprisingly, the impact on the algorithmic performance of (CUT) is much smaller. In fact, in several cases the reduced instances are even harder to solve. As mentioned above the optimal solutions remain the same as for the original instances. Therefore, we "lose" constraints that might help to prove optimality earlier. This is particularly relevant to the (CUT) model where the number of variables is independent of the number of the commodity pairs. As before, one solution obtained from (CH1+) is shown to be optimal and all but one of the remaining upper bounds from (CH1+) are improved by our approaches.

Sensitivity Analysis. The number of feasible walks realizing a connection of some commodity pair depends on the distance limit in relation to the edge lengths. More specifically, it depends on the average number of edges that can be part of a feasible subwalk that uses no relays. In the following, we want to investigate the effect of this characteristic on our algorithms. To this end, we consider the Cabral instances and vary the distance limit $d_{\max}$.

The unmodified Cabral instances feature a distance limit of 70 and the edge lengths are chosen uniformly at random from the interval $[10, 30]$. Therefore, a feasible walk of maximal length consists on average of three to four edges. Increasing $d_{\max}$ by a value of 30 means that a feasible walk without relays may contain at least one additional edge. We consider distance limits between

Figure 10. Sensitivity Analysis Regarding the Distance Maximum $d_{\max}$ on the Cabral Instances for the (CUT) Model

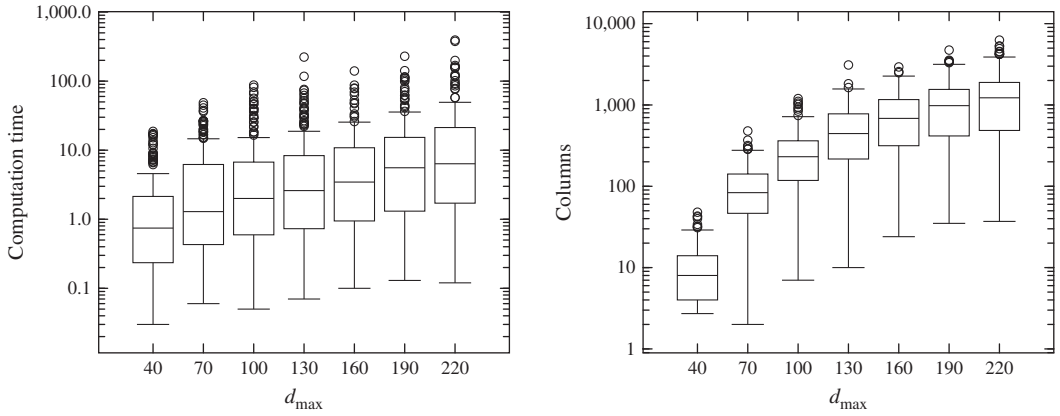

Notes. Each box considers 180 instances. Both box plots use a logarithmic scale.

40 and 220 in steps of 30 for our experiment. The results are visualized in terms of box plots in Figure 10 for the (CUT) model.

Because of the increasing number of possible options for connecting the commodity pairs, it can be expected that the instances become harder to solve as the distance limit increases. This can be verified in terms of the box plots. However, we can also see that the computing times increase only moderately. Per step, the median computing time rises by roughly one second. Similarly, the number of columns required to solve an instance to optimality increases. The respective results obtained with the (MCF) model are quite similar except that the baseline lies a bit higher. In total, we can conclude that the performance of our algorithms remains quite robust against changes to the distance limit.

Solution Shape and Characteristics. In this section, we analyze the structure of optimal solutions for two small examples corresponding to instances `40N30C50L20F_A` and `40N30C50L80F_A` from the ARLP set with 20% and 80% of free edges, respectively. In Figures 11(a) and 12(a) we visualize the two corresponding optimal solutions. We notice that for `40N30C50L20F_A`, despite the fact that there are 724 commodities, only three relays need to be installed (with a reasonable complement of augmentation edges) to enable these communications. In Figure 11, we compare the optimal solution of `40N30C50L20F_A` with the one obtained for the same input graph, but with a much smaller number of commodities: the set of commodities $\mathcal{K}'$ is obtained by removing all commodities except those containing the node that is involved in the fewest commodities.

Figure 11. (Color online) Solutions to ARLP Instance 40N30C50L20F_A with Different Numbers of Commodities

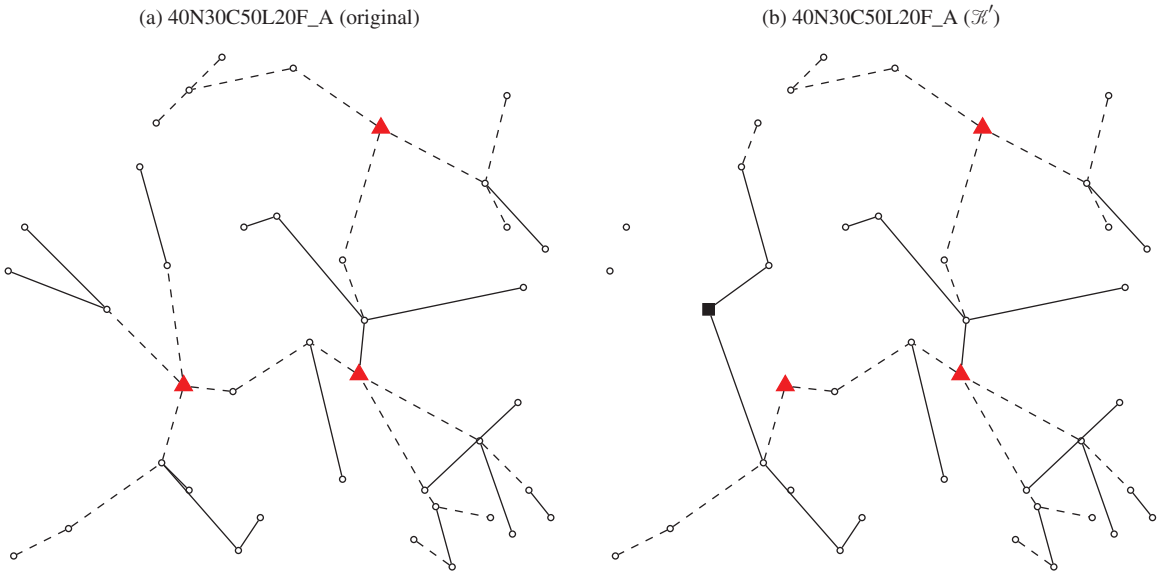

Notes. Solid lines indicate free edges and dashed lines augmenting edges. Selected relays are marked with triangles. On the right the single source is marked with a square.

Figure 12. (Color online) Solutions to ARLP Instance 40N30C50L80F_A with Different Numbers of Commodities

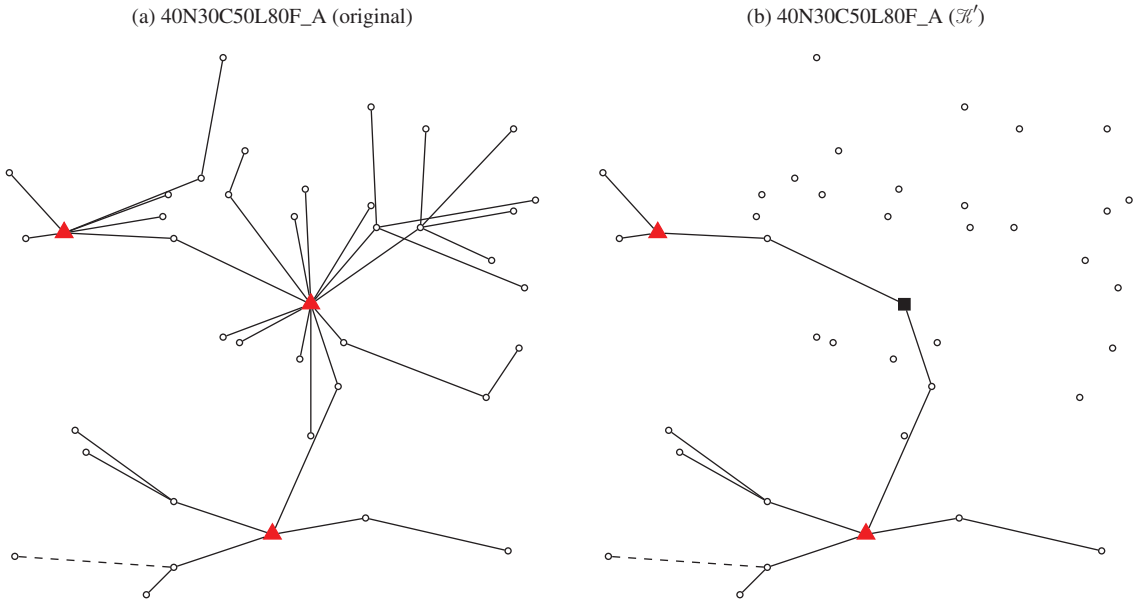

Notes. Solid lines indicate free edges and dashed lines augmenting edges. Selected relays are marked with triangles. On the right the single source is marked with a square.

The structure of the obtained optimal solution is similar to the original one, with three installed relays and a similar number of augmentation edges. Along with the results reported for the ARLP instances, this figure indicates that the estimated investment costs do not increase linearly with the number of commodities. In general there are higher investment costs for setting up the infrastructure, and once it is established, marginal increase in the number of commodities will not be reflected in the increase of the set-up costs (cf. the solution values in Tables 5 and 6).

Figure 12 visualizes the optimal solutions for `40N30C50L80F_A` and its "sparser" variant (with the set of commodities $\mathcal{K}'$ constructed as above), respectively. We observe that when 80 % of available edges are free, the need to install augmentation edges almost vanishes but a certain number of relays still needs to be installed to enable communications. Comparing the optimal solution for the sparser problem with the original one, we notice that the number of relays can be reduced, if the source node is centrally located, as this is the case in the shown example.

6. Conclusion

In this work we introduced new MILP formulations for the solution of the NDPR utilizing an exponential number of variables (and constraints). We proved several conditions and properties of optimal solutions and revised the concept of communication graphs for the NDPR that are exploited in our MILP formulations. Two branch-price-and-cut algorithms have been developed. The first one is based on a multicommodity flow formulation on an undirected communication graph, whereas the second is based on a cut-set formulation on a directed communication graph. The computational study on instances from the literature and a newly created set of instances shows that the cut-set formulation on the directed communication graph has the overall best performance. The multicommodity flow formulation on the undirected communication graph performs reasonably well, but only up to a limited number of nodes and/or commodities. Due to its excessive number of variables, the latter formulation exhibits serious memory issues that make it less appealing for practical applications involving larger graphs or a higher number of commodities.

We conducted a sensitivity analysis on the Cabral instances with different $d_{\max}$ restrictions. The results showed that our algorithms are quite robust against changes to this parameter featuring only a comparatively small increase in computing times and priced columns.

Compared to the previous attempt from the literature to develop an exact model for the NDPR by Cabral et al. (2007), the main advantage of our modeling approach is that we do not use variables corresponding to entire walks between commodities (including the decisions for placing relays). Instead, we consider only simple paths between two consecutive relays, whereas the decision where to place the relays is modeled through the communication graph. That way, our pricing draws a computational advantage from the fact that augmenting edges can be simultaneously shared by

multiple commodities. The positive effect of our modeling approach is striking for instances with many commodities, where the need for the simultaneous reuse of augmenting edges is even more amplified.

6.1. Future Work

Besides telecommunication network design, the NDPR can be used to answer strategic questions in the context of electric mobility. A company running its operations based on a fleet of electric vehicles (EVs), be it a logistics company or an e-car provider, faces a difficult decision problem of planning the underlying charging infrastructure. Due to expensive EV batteries and their limited range, a stable and robust charging infrastructure is crucial for running the business suitably. Since building and/or renting charging stations is expensive, logistic companies or e-car providers are interested in minimizing the number of charging stations whilst enabling travel between specific locations (cf. commodities). Furthermore, in some metropolises (including Stockholm, Gothenburg, and Singapore) *congestion taxing* or *congestion charging* mechanisms are implemented. This means that shorter distances can be traversed (e.g., via shortcuts through the inner city), but in that case a certain road toll is to be paid.[1,2] Similarly, urban freeways passing through a downtown area can be subject to compulsory electronic toll (like the case in Santiago de Chile, or some Norwegian cities). Consequently, if a company is interested in building charging stations for its fleet, it also has to gauge whether toll roads are to be used. When making strategic decisions, costs for toll roads are typically estimated over a longer planning period and considered as fixed link costs.

Two main strategic design questions arising in this complex decision process are addressed by the NDPR: Given a family of origin-destination pairs EVs need to travel, and given the existing links that can be traversed:

1. What are the optimal locations for placing the charging stations and how many of them are needed?

2. Could the available infrastructure be enhanced by including additional links (shortcuts), to reduce the travel distances?

The relevance of the NDPR for planning EVs' charging infrastructure has not been sufficiently acknowledged in the existing literature. This is maybe because of the additional aspects that need to be taken into account when dealing with e-mobility. These include restricting the distance arising from detours necessary for vehicle recharging and the maximum number of (time-consuming) recharging stops an EV requires before reaching its final destination. Although the NDPR does not consider these additional aspects, there is no doubt that the problem plays an important role for e-mobility applications for two reasons: (1) NDPR may appear as a subproblem (i.e., in some decomposition schemes), and (2) the proposed algorithms can be used to derive heuristic solutions in multiple-phase approaches, where the complex decision process is approached step by step. Hence, the NDPR provides important insights for the companies running their business with a fleet of EVs. It helps in estimating the initial set-up costs (induced by the installation of recharging stations and potential purchases of road-toll passes). Moreover, by using a correlation between the edge lengths and lengths of the trips, the routing decisions obtained through an NDPR solution implicitly help in estimating a lower bound on the number of required EVs. Similarly, assuming that all trips will be covered, an upper bound on the expected profit can be calculated.

Interesting and more difficult NDPR variants that are important directions for future work include the following aspects: (1) limiting the maximum number of recharging stops (relays) used by a single commodity, (2) limiting the maximum waiting times imposed by recharging, or (3) limiting the overall trip length per commodity.

Acknowledgments

The authors are grateful to the authors of Cabral et al. (2007) for providing their instance generator. Part of this research has been performed while M. Leitner was a research fellow at the Department of Computer Science, Université Libre de Bruxelles (Brussels, Belgium) where he was supported by the Interuniversity Attraction Poles Programme initiated by the Belgian Science Policy Office. This support is greatly acknowledged.

Endnotes

[1] https://www.epass24.com/ (accessed 2015-08-02).

[2] http://www.lta.gov.sg/content/ltaweb/en/roads-and-motoring/managing-traffic-and-congestion/electronic-road-pricing-erp.html (accessed 2015-08-02).

References

A21 Arslan O, Yıldız B, Karaşan OE (2015) Minimum cost path problem for plug-in hybrid electric vehicles. *Transportation Res. Part E: Logist. Transportation Rev.* 80:123–141.

Barnhart C, Johnson EL, Nemhauser GL, Savelsbergh MWP, Vance PH (1998) Branch-and-price: Column generation for solving huge integer programs. *Oper. Res.* 46(3):316–329.

BGL (2016) The boost graph library (BGL). Accessed September 9, 2017, http://www.boost.org/doc/libs/1_63_0/libs/graph/doc/index.html.

Cabral EA, Erkut E, Laporte G, Patterson RA (2007) The network design problem with relays. *Eur. J. Oper. Res.* 180(2):834–844.

Campbell JF, O'Kelly ME (2012) Twenty-five years of hub location research. *Transportation Sci.* 46(2):153–169.

Capar I, Kuby M, Leon VJ, Tsai Y-J (2013) An arc cover–path-cover formulation and strategic analysis of alternative-fuel station locations. *Eur. J. Oper. Res.* 227(1):142–151.

Chen S, Ljubić I, Raghavan S (2010) The regenerator location problem. *Networks* 55(3):205–220.

Chen S, Ljubić I, Raghavan S (2015) The generalized regenerator location problem. *INFORMS J. Comput.* 27(2):204–220.

A22 Cherkassy BV, Goldberg AV (1995) On implementing push-relabel method for the maximum flow problem. *Proc. 4th Internat. IPCO Conf. Integer Programming Combin. Optim.* (Springer), 157–171.

Desrosiers J, Lübbecke ME (2011) Branch-price-and-cut algorithms. *Wiley Encyclopedia of Operations Research and Management Science* (John Wiley & Sons, Hoboken, NJ).

Dijkstra EW (1959) A note on two problems in connexion with graphs. *Numerische Mathematik* 1(1):269–271.

Gamrath G, Fischer T, Gally T, Gleixner AM, Hendel G, Koch T, Maher SJ, et. al (2016) The SCIP optimization suite 3.2. Technical Report 15-60, ZIB, Berlin.

Gendron B, Lucena A, da Cunha AS, Simonetti L (2014) Benders decomposition, branch-and-cut, and hybrid algorithms for the minimum connected dominating set problem. *INFORMS J. Comput.* 26(4):645–657.

A23 Kabadurmus O, Smith AE (2015) Multi-commodity k-splittable survivable network design problems with relays. *Telecomm. Systems* 1–11.

Konak A (2012) Network design problem with relays: A genetic algorithm with a path-based crossover and a set covering formulation. *Eur. J. Oper. Res.* 218(3):829–837.

A24 Kulturel-Konak S, Konak A (2008) A local search hybrid genetic algorithm approach to the network design problem with relay stations. Raghavan S, Golden B, Wasil E, eds. *Telecommunications Modeling, Policy, and Technology*. Operations Research/Computer Science Interfaces, Vol. 44 (Springer), 311–324.

Laporte G, Pascoal MMB (2011) Minimum cost path problems with relays. *Comput. Oper. Res.* 38(1):165–173.

Li X, Aneja YP, Huo J (2012) Using branch-and-price approach to solve the directed network design problem with relays. *Omega* 40(5):672–679.

A25 Lin S, Li X, Wei K, Yue C (2014) A tabu search based metaheuristic for the network design problem with relays. *Service Systems and Service Management (ICSSSM), 2014 11th Internat. Conf.*, 1–6.

Ljubić I, Weiskircher R, Pferschy U, Klau GW, Mutzel P, Fischetti M (2006) An algorithmic framework for the exact solution of the prize-collecting Steiner tree problem. *Math. Program.* 105(2–3): 427–449.

Lucena A, Maculan N, Simonetti L (2010) Reformulations and solution algorithms for the maximum leaf spanning tree problem. *Comput. Management Sci.* 7(3):289–311.

Pelletier S, Jabali O, Laporte G (2016) 50th anniversary invited article—Goods distribution with electric vehicles: Review and research perspectives. *Transportation Sci.* 50(1):3–22.

Raghavan S, Stanojević D (2011) Branch and price for WDM optical networks with no bifurcation of flow. *INFORMS J. Comput.* 23(1):56–74.

A26 Rahman Q, Bandyopadhyay S, Aneja Y (2015) Optimal regenerator placement in translucent optical networks. *Optical Switching Networking* 15:134–147.

Schneider M, Stenger A, Goeke D (2014) The electric vehicle-routing problem with time windows and recharging stations. *Transportation Sci.* 48(4):500–520.

Sung CS, Song SH (2003) Branch-and-price algorithm for a combined problem of virtual path establishment and traffic packet routing in a layered communication network. *J. Oper. Res. Soc.* 54(1): 72–82.

Üster H, Kewcharoenwong P (2011) Strategic design and analysis of a relay network in truckload transportation. *Transportation Sci.* 45(4):505–523.

Üster H, Maheshwari N (2007) Strategic network design for multizone truckload shipments. *IIE Trans.* 39(2):177–189.

A27 Xiao Y, Konak A (2017) A variable neighborhood search for the network design problem with relays. *J. Heuristics* 1–28.

A28 Yıldız B, Karaşan OE (2015) Regenerator location problem and survivable extensions: A hub covering location perspective. *Transportation Res. Part B: Methodological* 71:32–55.

Yıldız B, Karaşan OE (2017) Regenerator location problem in flexible optical networks. *Oper. Res.* 65(3):595–620.

Yıldız B, Arslan O, Karaşan OE (2016) A branch and price approach for routing and refueling station location model. *Eur. J. Oper. Res.* 248(3):815–826.

A29 Yıldız B, Karaşan OE, Yaman H (2018) Branch-and-price approaches for the network design problem with relays. *Comput. Oper. Res.* 92:155–169.

Author Queries

A1 Au: Please confirm names, affiliations, and email addresses are okay as set. Provide author(s) ORCID number(s) if applicable.

A2 Au: Please confirm keywords.

A3 Au: Please confirm heading levels are correct.

A4 Au: Set all section 1 subsections as numbered 2-heads as per style? Please check here and throughout the text (which subsections should be revised to 2-heads or 4-heads is not clear). Per style, if main sections are numbered, all subsections should be numbered.

A5 Au: Please check that all figures and tables are set correctly.

A6 Au: In Figures 1, 2, 4–12, and Tables 1–6, we have maintained first sentence alone as caption and rest as notes. Kindly check.

A7 Au: Please provide specific section number.

A8 Au: Color figures will be converted to grayscale for the print version unless color in print has been requested and paid for. Authors have the responsibility to check that the figures are sufficiently clear in both the online color and print black and white versions.

A9 Au: Add specific section numbers

A10 Au: Please verify that all equations are set correctly.

A11 Au: Revise as numbered 4-head under 3.2 (3.2.1)?

A12 Au: No "forall" here – there is no statement to act on.

A13 Au: Revise to numbered 4-head 3.3.1?

A14 Au: What is the relation to the line above?

A15 Au: "Forall" is acting here on the set. Do you mean $\forall(i, j)$, $\{i, j\} \in E^*$.

A16 Au: Please provide specific section number here.

A17 Au: What is this breve accent doing here? Please clarify.

A18 Au: Set section 4.2, 4.3, and 5.1 subsubsections as numbered 4-heads as per style? Please check.

A19 Au: Set a period at the end of the algorithm? Please check.

A20 Au: Revised to "four-grid" OK?

A21 Au: Please include issue number.

A22 Au: Please include editors, and location for Springer.

A23 Au: Please include volume and issue numbers.

A24 Au: Please include specific Springer city/state location, not US.

A25 Au: Please include editors and name and location of the publisher, or location of conference.

A26 Au: Please include issue number.

A27 Au: Please include volume and issue numbers.

A28 Au: Please include issue number.

A29 Au: Please include issue number.